

## SCIENCE OF TSUNAMI HAZARDS

Journal of Tsunami Society International

Volume 31

Number 4

2012

---

### EARLY DETECTION OF NEAR-FIELD TSUNAMIS USING UNDERWATER SENSOR NETWORKS 231

**L. K. Comfort, T. Znati, M. Voortman, and Xerandy** - *University of Pittsburgh, USA*  
**L. E. Freitag** - *Woods Hole Oceanographic Institution, USA*

### TSUNAMI MITIGATION PLANNING IN PACITAN, INDONESIA: A REVIEW OF EXISTING EFFORTS AND WAYS AHEAD 244

**A. Muhari**

*Ministry of Marine Affairs and Fisheries (KKP), Jakarta 10110, INDONESIA*  
*Disaster Control Research Center, Tohoku University, Sendai 980-8579, JAPAN*

**M. Mück**

*German Remote Sensing Data Center (DFD), German Aerospace Center (DLR), Wessling, GERMANY*

**S. Diposaptono** - *Ministry of Marine Affairs and Fisheries (KKP), Jakarta 10110, INDONESIA*

**H. Spahn** - *GIZ International Services, Jakarta 10310, INDONESIA*

### THE TOHOKU TSUNAMI OF 11 MARCH 2011 AS RECORDED ON THE RUSSIAN FAR EAST 268

**G. V. Shevchenko** - *Institute of Marine Geology and Geophysics FEB RAS, Yuzhno-Sakhalinsk, RUSSIA*

**T. N. Ivelskaya** - *Sakhalin Tsunami Warning Center, Yuzhno-Sakhalinsk, RUSSIA*

### RESPONSE OF THE GDACS SYSTEM TO THE TOHOKU EARTHQUAKE AND TSUNAMI OF 11 MARCH 2011 283

**Annunziato, G. Franchello, T. De Groeve** - *EC-Joint Research Centre (EC-JRC), Ispra, ITALY*

*Copyright © 2012 - TSUNAMI SOCIETY INTERNATIONAL*

[WWW.TSUNAMISOCIETY.ORG](http://WWW.TSUNAMISOCIETY.ORG)

***TSUNAMI SOCIETY INTERNATIONAL, 1741 Ala Moana Blvd. #70, Honolulu, HI 96815, USA.***

***SCIENCE OF TSUNAMI HAZARDS is a CERTIFIED OPEN ACCESS Journal included in the prestigious international academic journal database DOAJ, maintained by the University of Lund in Sweden with the support of the European Union. SCIENCE OF TSUNAMI HAZARDS is also preserved, archived and disseminated by the National Library, The Hague, NETHERLANDS, the Library of Congress, Washington D.C., USA, the Electronic Library of Los Alamos, National Laboratory, New Mexico, USA, the EBSCO Publishing databases and ELSEVIER Publishing in Amsterdam. The vast dissemination gives the journal additional global exposure and readership in 90% of the academic institutions worldwide, including nationwide access to databases in more than 70 countries.***

**OBJECTIVE:** Tsunami Society International publishes this interdisciplinary journal to increase and disseminate knowledge about tsunamis and their hazards.

**DISCLAIMER:** Although the articles in SCIENCE OF TSUNAMI HAZARDS have been technically reviewed by peers, Tsunami Society International is not responsible for the veracity of any statement, opinion or consequences.

#### **EDITORIAL STAFF**

Dr. George Pararas-Carayannis, Editor  
<mailto:drgeorgepc@yahoo.com>

#### **EDITORIAL BOARD**

Dr. Charles MADER, Mader Consulting Co., Colorado, New Mexico, Hawaii, USA  
Dr. Hermann FRITZ, Georgia Institute of Technology, USA  
Prof. George CURTIS, University of Hawaii -Hilo, USA  
Dr. Tad S. MURTY, University of Ottawa, CANADA  
Dr. Zygmunt KOWALIK, University of Alaska, USA  
Dr. Galen GISLER, NORWAY  
Prof. Kam Tim CHAU, Hong Kong Polytechnic University, HONG KONG  
Dr. Jochen BUNDSCHUH, (ICE) COSTA RICA, Royal Institute of Technology, SWEDEN  
Dr. Yuri SHOKIN, Novosibirsk, RUSSIAN FEDERATION

#### **TSUNAMI SOCIETY INTERNATIONAL, OFFICERS**

Dr. George Pararas-Carayannis, President;  
Dr. Tad Murty, Vice President;  
Dr. Carolyn Forbes, Secretary/Treasurer.

Submit manuscripts of research papers, notes or letters to the Editor. If a research paper is accepted for publication the author(s) must submit a scan-ready manuscript, a Doc, TeX or a PDF file in the journal format. Issues of the journal are published electronically in PDF format. There is a minimal publication fee for authors who are members of Tsunami Society International for three years and slightly higher for non-members. Tsunami Society International members are notified by e-mail when a new issue is available. Permission to use figures, tables and brief excerpts from this journal in scientific and educational works is granted provided that the source is acknowledged.

Recent and all past journal issues are available at: <http://www.TsunamiSociety.org> CD-ROMs of past volumes may be purchased by contacting Tsunami Society International at [postmaster@tsunamisociety.org](mailto:postmaster@tsunamisociety.org) Issues of the journal from 1982 thru 2005 are also available in PDF format at the Los Alamos National Laboratory Library <http://epubs.lanl.gov/tsunami/>



**EARLY DETECTION OF NEAR-FIELD TSUNAMIS USING UNDERWATER SENSOR NETWORKS**

**L. K. Comfort, T. Znati, M. Voortman, and Xerandy,**

*University of Pittsburgh, USA*

**L. E. Freitag,**

*Woods Hole Oceanographic Institution, USA*

**ABSTRACT**

We propose a novel approach for near-field tsunami detection, specifically for the area near the city of Padang, Indonesia. Padang is located on the western shore of Sumatra, directly across from the Mentawai segment of the Sunda Trench, where accumulated strain has not been released since the great earthquake of 1797. Consequently, the risk of a major tsunamigenic earthquake on this segment is high. Currently, no ocean-bottom pressure sensors are deployed in the Mentawai basin to provide a definitive tsunami warning for Padang. Timely warnings are essential to initiate evacuation procedures and minimize loss of human life. Our approach augments existing technology with a network of underwater sensors to detect tsunamis generated by an earthquake or landslide fast enough to provide at least 15 minutes of warning. Data from the underwater sensor network would feed into existing decision support systems that accept input from land and sea-based sensors and provide warning information to city and regional authorities.

## 1. PROBLEM STATEMENT

The threat of *near-field tsunamis* represents a significant risk for coastal communities located near earthquake subduction zones, and it is particularly high along the west coast of Sumatra, Indonesia. In a recent paper in *Nature Geoscience*, J. McCloskey et. al. (2010) noted that the 2009 Padang Earthquake had not ruptured the Mentawai segment of the Sunda Trench, and that the accumulated strain of more than 200 years represented high potential for a major tsunamigenic earthquake that would threaten the cities of Padang and Bengkulu on the western coast of Sumatra.

The threat is different than that posed by distant tsunamis in that the warning time is much less and detection must occur close to the affected area. The DART system has achieved significant success in detecting tsunamis that originate far away (offshore on or near other continents), but it has three key limitations. First, due to their primary function, the DART buoys are anchored at least 250 miles off shore and therefore do not generally detect near-field tsunamis for the coasts they protect. Second, the cost of building, deploying, and maintaining a network of DART buoys is high, and places a heavy financial burden on developing nations such as Indonesia. Third, as Indonesia has deployed a network of DART buoys for both near- and far-field tsunami detection, BPPT (Agency for Assessment and Application of Technology) has reported that vandalism is a consistent problem, reducing the number of buoys that can be maintained. At a recent visit to the BPPT engineering laboratory in Puspitek Serpong, Senior Scientist Wahyu Pandoe stated that of 19 sites established by BPPT for DART buoys on the coasts of Indonesia, only 4 were populated by operating buoys, after repeated instances of vandalism.<sup>1</sup> Given this situation, BPPT is seeking alternative methods for tsunami detection, which obviate or reduce the need for near-shore buoys.

## 2. GOAL OF RESEARCH

This paper describes a new approach for telemetering data to allow detection of near-field tsunamis without the use of surface buoys. The system would be located off the shore of Padang, Sumatra, Indonesia (Figure 1). The work focuses specifically on the design of an underwater sensor network, the most technically challenging component. If a demonstration system proves successful, the network would be connected to the existing land-based Indonesian Tsunami Early Warning System (TEWS).

In addition the data from this network may feed into a land-based model that could estimate the impact of a tsunami on the built infrastructure and population of a city at risk. The design and development of the land-based model and the associated dynamic Geographic Information Systems that present the model outputs to users are additional components of an end-to-end tsunami detection system, but both are beyond the scope of this paper. The land-based model was addressed briefly in a

---

<sup>1</sup> Personal communication, BPPT Facility, Serpong, Indonesia, July 10, 2012.

previous paper (Boulos et al., 2012) and the dynamic GIS functions will be addressed in subsequent work.

Designing, building, and testing an experimental system to address this threat would help to address a gap in near-field tsunami detection and warning research that will help coastal communities. Recent events have highlighted the importance of this problem, notably the December 26, 2004 Sumatran Earthquake and Tsunami; February 27, 2010 Chile Earthquake and Tsunami; October 25, 2010 Mentawai, Indonesia Tsunami; and March 11, 2011 Tohoku, Japan Earthquake, Tsunami, and Nuclear Reactor Breach.

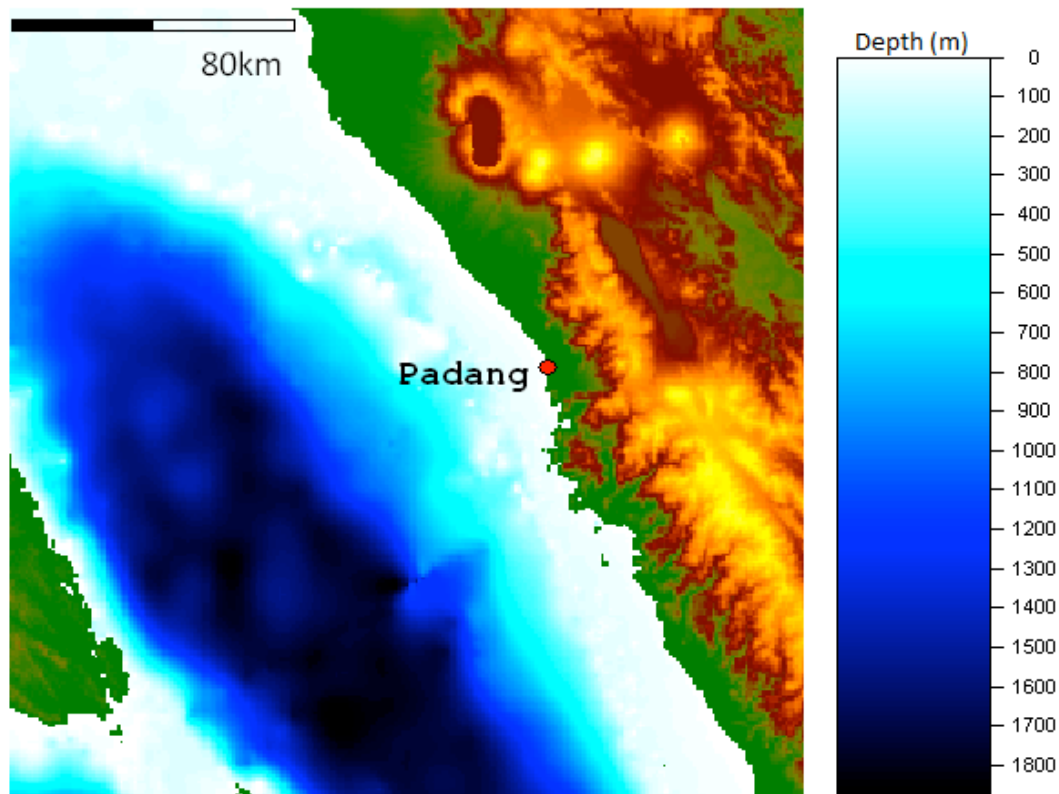


**Figure 1.** Map of study region showing ocean depth in meters offshore Padang, Sumatra

### 3. ESTIMATING TSUNAMI PARAMETERS

Tsunami warning systems, as currently deployed, are challenged by the simple fact that near-field tsunamis strike so quickly (Strunz et al, 2011; Lauterjung et al, 2010). Prediction of wave propagation has been greatly advanced by Titov et al. (2003), who developed the Method of Splitting Tsunami (MOST) model, which is used extensively throughout the international community, including the US National Oceanic, and Atmospheric Administration (Morrissey, 2005). This model includes elements

that estimate the fault plane parameters and sea-floor displacement to then generate the initial conditions for the tsunami wave. As implemented at National Oceanic and Atmospheric Administration (NOAA) Pacific Marine and Environmental Laboratory (PMEL), the codes then estimate propagation through the ocean, and finally, the inundation that may result. Ocean-bottom pressure sensor data from the DART buoys (Bernard et al., 2006; Satake, Okal, and Borrero, 2007) are used to refine the initial conditions and propagation estimates.

Methods for quickly and accurately estimating earthquake magnitude and sea floor displacement continue to be refined with the goal of improving tsunami prediction. As networks of real-time GPS stations expand and fault plane parameter calculation improves in accuracy and speed, the estimation of tsunami magnitude may improve. Work on use of W-phase to compute  $M_w$  may provide a faster estimate of earthquake moment (Singh et al., 2012) that may then be used for tsunami parameter calculation. It has also been proposed that appropriately-located real-time GPS stations on Sumatra and its offshore islands could provide estimates of co seismic slip and consequently improve tsunami warnings (Behrens, 2010).

*However, ocean-bottom pressure sensors offer definitive measurements that when coupled with propagation models can provide accurate inundation information.* Unfortunately, due to vandalism (UNESCO, 2011) and the maintenance issues alluded to above, a near-shore, buoy-based approach to telemeter ocean bottom pressure data (or host real-time kinematic GPS, another sea-based measurement), is not practical for Indonesia.

## **4. TECHNICAL APPROACH**

### **4.1 Bottom Sensor**

A bottom pressure signal indicating the magnitude of a tsunami wave well away from shore would be a significant addition to the Indonesian TEWS for western Sumatra. As noted above, the bottom pressure sensor provides an unambiguous measurement (e.g. Figure 2) that can be directly extrapolated to compute the height and time of arrival of the tsunami. However, an additional complication arises when the pressure sensor is near the earthquake source: the seismic signal is also detected by the sensor. This is not a significant issue when the pressure sensor and earthquake source are widely separated because the early signal on the pressure sensor can be identified as being seismically generated. However, it must be addressed when both are present at the same time on the pressure sensor.

Fortunately, a recent development by Paroscientific, the primary manufacturer of ocean-bottom pressure sensors used for tsunami detection, has resulted in an enhanced instrument, a nano-resolution sensor that may allow separation of earthquake vibrations and low-level pressure signals (Paros et al, 2011). The nano-resolution sensor is not significantly more expensive than the standard sensor (about 20% more), and it is capable of measuring 1 mm signals in deep water. The capability of the instrument is currently being tested in Monterey Bay, California with support by the US National Science Foundation. The sensor will ultimately be used on the permanent regional cabled observatory

to be installed in the Pacific Ocean off the Washington and Oregon coasts where near-field tsunami risk is also present.

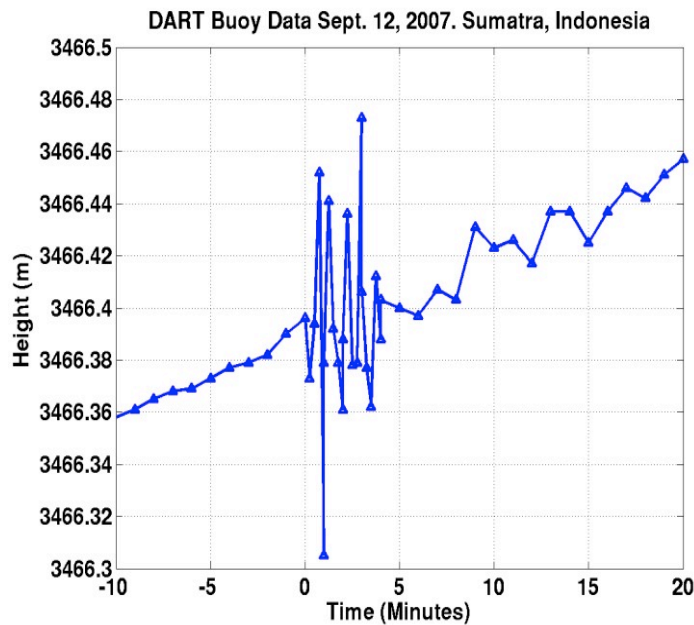


**Figure 2.** Pressure data recorded by a DART (r) buoy during the Sumatra tsunami event of Sept. 12, 2007. (Data from NOAA).

Work remains to develop and validate an algorithm that unambiguously detects a tsunami pressure signal in the presence of contaminating motion-generated data. However, co-located accelerometers may provide a means of disambiguation, though at additional cost and complexity.

#### 4.2 Proposed Undersea Acoustic Network

While the US and Japan have the capability and funding to install cables for deep-water observatories to host ocean sensors, the costs are extremely high and impractical for Indonesia at present. Thus an alternative method to both long cables and buoys is needed, and it is proposed that acoustic communications may provide a solution for the near-term.

Undersea acoustic communications is a maturing field, in particular for near-vertical links from the sea floor to the surface as in the DART buoy case (Meinig et al., 2005). However, long-range acoustic communications methods are also feasible, albeit at lower bit rates and higher cost per bit in energy than verticals links that are typically less than 6-8 km. Acoustic communication over ranges of 20-30 km has been demonstrated in other contexts (Freitag et al., 2000), so it is logical to ask whether such systems could be applied to the problem described here: transporting pressure data to shore with a minimum of cabled infrastructure. While a detailed description of how sound travels in the ocean is

beyond the scope of this paper, it suffices to note that it does not travel in a straight line, but rather bends due to changes in density, which affect the speed of sound. Warm surface water is faster than deeper, colder water, though as pressure increases with depth, sound ultimately travels faster at the bottom than at the surface.

In equatorial areas such as Indonesia, the surface water is very warm and the temperature is relatively constant throughout the seasons. As sound transmitted from the bottom approaches the surface, at a certain critical angle it will fully refract, bending away from the surface and never striking it. The lack of surface interaction eliminates the scatter that would otherwise reduce the signal level and distort it, and thus creates the propagation conditions that will be exploited in the proposed system: bottom-to-bottom communications links that may be used to build an underwater sensor network. The effect is illustrated in Figure 3. Here a model of transmission loss from a sound source on the bottom is shown, using sound speed derived from archival temperature, conductivity and pressure data to perform the computations. The effect described here is clearly visible, the sound bends away from the surface, returning to the bottom at ranges of 15 to 45 km.

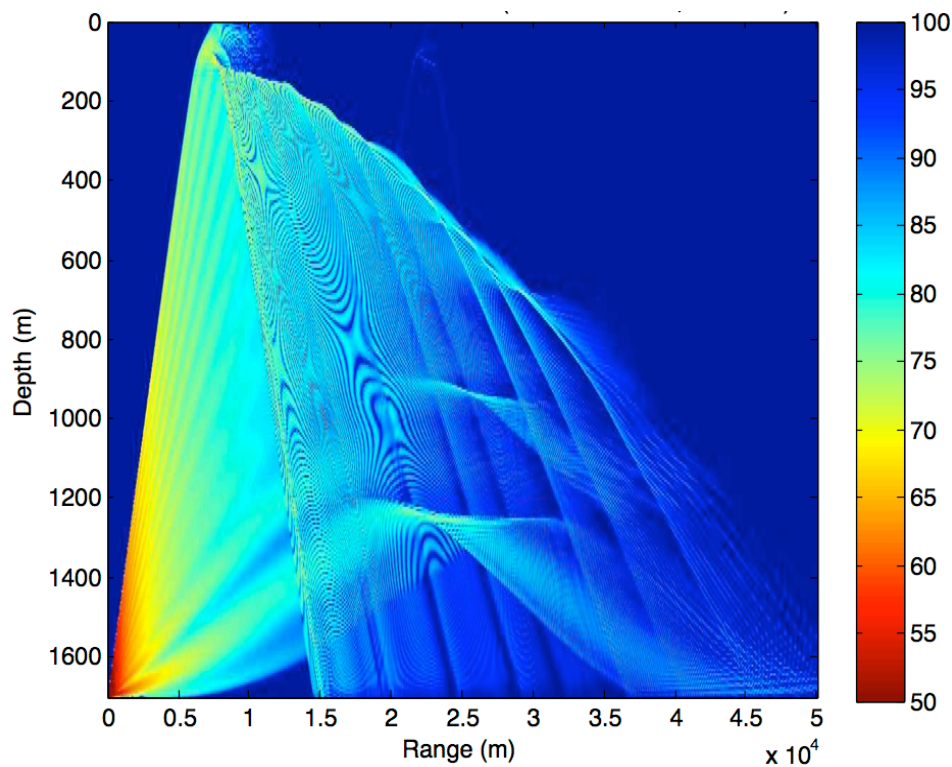


**Figure 3.** Modeled transmission loss of a signal sent from the bottom of the Mentawai Basin, which demonstrates how sound, refracts at the surface and returns to the bottom 15 to 45 km away (not all angles are shown).

While the existence of these acoustic propagation conditions implies that communications using an acoustic modem is possible, many questions remain regarding its configuration, including the number of hops and the use of relay nodes to increase the size of the network. For example, longer links can be established by using more energy per bit of information, but multiple hops at shorter ranges (for example, 20 km), could allow adding additional sensors to increase redundancy. These and other trade-offs are examined within the framework of a simple network design model in the following section.

### 4.3 Design parameters for the underwater sensor network

Designing the underwater sensor network requires determining the key parameters for the network and the possible trade-offs in cost, efficiency, and robustness among them. Given the objective of the network to achieve at least 15 minutes of warning time between the detection of a tsunamigenic earthquake and the arrival of the wave on shore, several parameters in the network design can be varied, resulting in different balances of cost, efficiency, and robustness in an underwater sensor network. An overview of the design parameters is given in Figure 4.

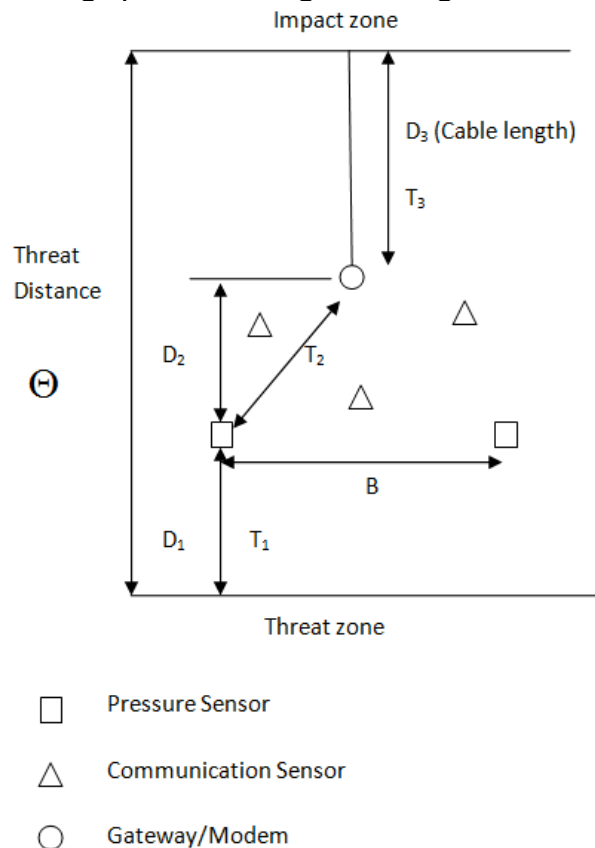


**Figure 4.** Design parameters for the underwater sensor network.

The design constraint for any functional sensor network can be expressed by the following equation:

$$\sum_{i=1}^3 T_i + T_p \leq \Theta - W$$

Where:

$T_1$  = Time for the tsunami wave to reach the pressure sensor, which is a complex function of sea depth, earthquake magnitude, and distance from the sensor.

$T_2$  = Time for acoustic wave to reach the acoustic modem, which is a function of the underwater acoustic channel propagation model, ocean temperature, and distance,  $D_1$ .

$T_3$  = Time for the optical signal to reach the land station, which is a function of the speed of light in fiber, and the distance,  $D_2$ .

$\Theta$  = Time for the tsunami wave to strike land, which is a function of the sea depth, earthquake magnitude, gravitational acceleration, and distance,  $D_3$ .

$T_p$  = Packet processing time at pressure sensor and acoustic modem.

$W$  = Warning time necessary for evacuation, for example, 15 minutes.

The threat zone is the area where an earthquake might occur, and the impact zone is the area we are trying to protect by giving out a timely warning. Given the impact zone and the threat zone, the threat distance is fixed and the time  $\Theta$  it will take the tsunami to travel from the threat zone to the impact zone depends on the bathymetry of the area between the zones.  $D_1$  is defined as the distance between the threat zone and the pressure sensors, and  $B$  is defined as the distance between specific pressure sensors. Bottom pressure sensors forward their measurements to a cable modem attached to the end of the optical fiber cable over a distance  $D_2$ , and this information is relayed through communication nodes, if necessary.  $D_3$  is the cable length. We first make our design constraint explicit before defining the remaining parameters.

The objective of the underwater sensor network is to achieve reliable, on-time delivery of data that detects the passing of a tsunami wave. Several factors could affect this model, resulting in different rates of transmission under different conditions. While the climatological data and propagation modeling described above indicate that the warm upper-layer water refracts sound away from the surface and back to the bottom, it is necessary to verify this and confirm the presence or absence of other propagation effects that may impact data rate and power efficiency. Any effects that are revealed by initial testing will need to be evaluated and taken into consideration in the final design of the underwater sensor network.

Our design of the sensor network will incorporate adaptive features of network communications technology to conserve energy, reduce error, and extend the operational capacity of the network. For

example, it will include adaptive automatic repeat-request (ARQ) protocols with minimal reliance on Request to Send/Clear to Send (RTS and CTS) mechanisms. Second, the communications network will include dynamic routing to overcome enduring failures in network transmission. This approach will identify relay points for path redundancy in transmission, while minimizing energy consumption. Third, the design will include in-network storage of data to overcome transient failures in transmission and improve network reliability. Fourth, the design will employ joint optimization of erasure codes and forward error correction protocols to minimize the impact of bit errors and packet loss in transmission. This will include calculating trade-offs in context, quality of data, and climate sensitivity to achieve optimum energy consumption while achieving high levels of reliability in accuracy and time.

Given the potential complexity of the underwater sensor network, with its spatial extent still in the design phase, we seek to test our assumptions and explore different options by using computational modeling to simulate the different alternatives. The results allow a comparative assessment of the optimum design for the underwater network, given the specific conditions of the Padang coastal environment. This approach will inform the development of a testbed that will allow systematic evaluation of different designs prior to a major investment in the deployment of a underwater sensor network.

#### **4.4 Optimizing design parameters**

The previous section explained which design parameters we take into account for the underwater sensor network. In this section, we evaluate and compare several different designs for Padang by running a computer program that takes as input the warning time and reliability, and then finds an optimal design in terms of cost. We also evaluate alternative designs by fixing some parameter, e.g., making the cable a fixed length, and then compare the alternatives to the optimal design.

Several parameters were determined prior to running the program. For Padang, we know in which areas earthquakes are likely to occur, so we can fix the threat zone. The impact zone will be the most densely populated area along the coast, which we estimated using maps available to us. If decision makers disagree with this estimate, it could easily be changed. Having these two zones fixed, we can estimate  $\Theta$ , which is the minimum time it would take for the wave to travel from the threat zone to the impact zone, by using bathymetry data and an approximation of the shallow water equations. Given the locations of our threat and impact zone, it will take about 28 minutes for the wave to reach the coastline. The propagation model for acoustic waves is very complicated, since it depends on the temperature, pressure (or depth), and salinity. The propagation model for channel loss and absorption is also very complicated, because it not only depends on distance, but also frequency and temperature. For these reasons, we used simple constants that approximate the real values for acoustic wave propagation. In future work we are planning to incorporate the real values.

It is important to emphasize that every design should satisfy  $\sum_{i=1}^3 T_i + T_p \leq \Theta - W$ , which is defined in the previous section, otherwise the warning may be too late. There could actually be many designs

that satisfy this criterion, which is why the program will simply return the design with the lowest cost to implement. When warning time  $W$  is set too high, it is possible that no design could satisfy the equation. Different designs also have different reliability levels. One approach to increase the reliability is to install more sensors and relay nodes because they provide backup and alternate communication routes. Deploying more devices, however, incurs more expenses.

We previously noted that alternative designs could be evaluated by fixing some of the parameters, such as the cable. In that setting, only the values of other parameters will be chosen that minimize the cost. This cost will never be less than the design without the fixed parameter, but in some cases policy makers may have a preference for a certain design parameter, and they would like to see how that parameter affects the cost. The cost function takes into account the cost for the pressure sensors, the communication sensors, the cable, and the deployment of the cable. The costs shown are relative to the Design 1 cost.

*Design 1:* This is the optimal design, i.e., the design with the lowest cost, but without any redundancy built in (low reliability).

*Design 2:* This is the same as design 1, but all the sensors are redundant so there is no single point of failure (high reliability).

*Design 3:* This is the same as design 2, but with a 20 km cable.

*Design 4:* This is the same as design 3, but with a 20 minute warning time.

The results of the different designs are listed in Table 1 below:

**Table 1. Comparison of Design Parameters for Underwater Sensor Network**

Parameter	Design 1	Design 2	Design 3	Design 4
W (warning time)	15	15	15	20
Reliability	Low	High	High	High
# of pressure sensors	1	2	2	2
# of communication nodes	2	4	4	4
$D_1$	68 km	54 km	32 km	43 km
$D_2$	17 km	29 km	37 km	37 km
$D_3$ (cable length)	4 km	7 km	20 km	9 km
Cost	N	1.8*N	3.2*N	2*N

The least expensive design does not have any redundancy built in. The design with redundancy is almost twice the cost, but is much safer, because there is no single point of failure. Since extending the cable is expensive, design 3 is by far the most costly. The fourth design gives some valuable insight into the design process. Note that the cable length has increased compared to designs 1 and 2 because a longer (optical fiber) cable means faster transmission than through the acoustic network, so the warning can be given earlier. Yet the design is much cheaper than design 3, which warrants a 15

minute warning time, but the reason is that the time constraint on the model is only a lower bound and, in fact, design 3 actually provides 22-minute warning time.

#### 4.5 Visualizing the Tsunami Warning Network

After identifying an optimal design, we would like to use it in a scenario and present it graphically to those involved in making design and policy decisions. In order to do that, we created an additional module that simulates an earthquake and subsequent events, including traffic through the different sections of the network. In Figure 4 below, the output of this module is shown on a map. The orange line is the threat zone and the red line is the impact zone. The blue line is the communication cable. An earthquake is simulated in the threat zone, which causes a tsunami to start traveling to the coast. The green lines show the location of the wave in one-minute increments. The wave has reached the pressure sensor, which has become active (colored red). This information has not been transmitted to the coast yet, because the gateway is still inactive (colored gray).

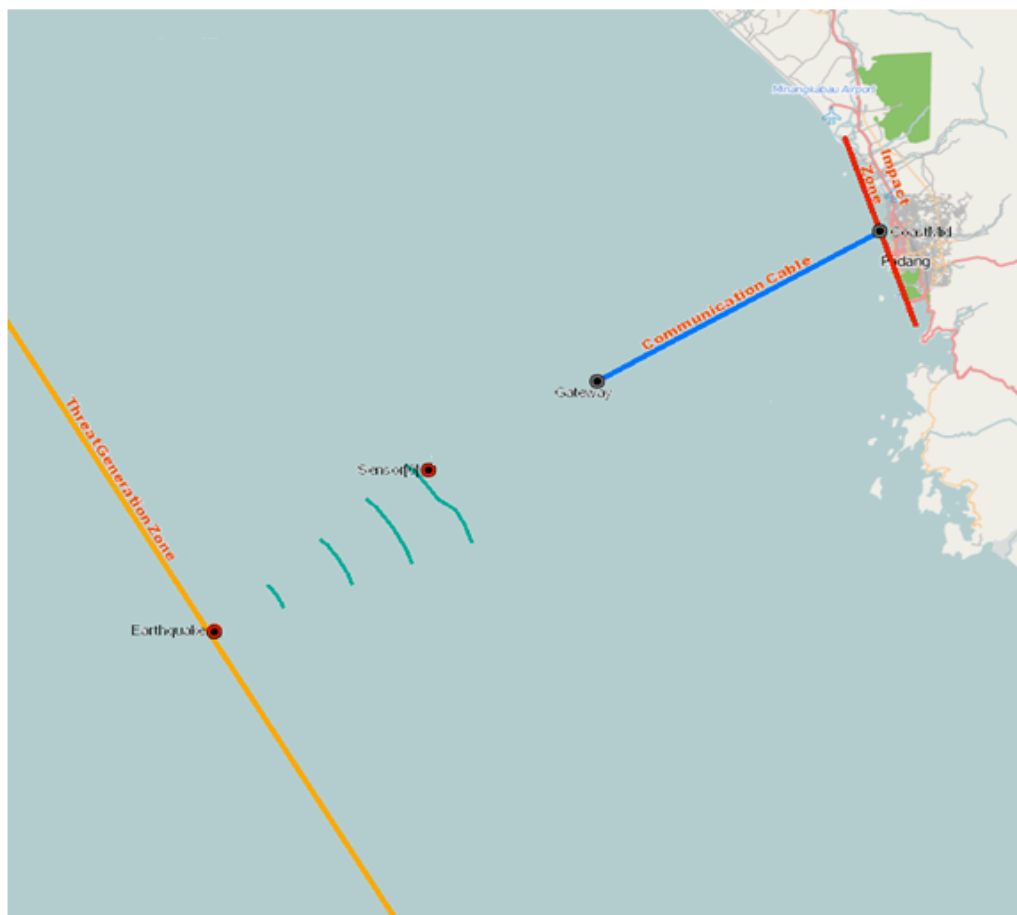


**Figure 4.** Computer simulation of tsunami wave propagation, detection by a sensor, and transmission through the acoustic and cable network for a particular scenario.

## 5. Conclusions

Four primary conclusions summarize the work described in this paper. First, near-field tsunami detection remains an important topic that warrants continued research into both methods and real-time data telemetry. Second, at the moment, ocean bottom pressure sensors offer the most practical means of detecting and then reliably estimating the magnitude of tsunamis. Third, warm ocean waters in equatorial environments create the effect of bending sound waves back to the bottom of the ocean floor, allowing acoustic communications to travel longer distances than would otherwise be possible from bottom sensors. This condition creates the basis for an underwater sensor network that could transmit tsunami detection data to a shore-connected receiving station with sufficient warning time (at least 15 minutes) to inform emergency managers who could mobilize evacuation strategies for communities at risk. Fourth, such a sensor network, such as described here in model form, requires prototyping and testing in an actual ocean environment to determine the optimal design, using metrics that include cost, efficiency, and robustness before making a major investment. If validated through such a demonstration project, this approach could benefit hundreds of thousands of people who live in coastal communities at risk from tsunamis. While the proposed solution is motivated by the difficulty in maintaining buoys near shore in Indonesia due to vandalism, it may find uses in other environments as well where the acoustic system can connect to existing or planned subsea ocean observatories.

## ACKNOWLEDGEMENTS

We acknowledge, with thanks and appreciation, financial support from the U.S. National Science Foundation, Decision, Risk, and Uncertainty grant #0729456, institutional support of the University of Pittsburgh, Woods Hole Oceanographic Institution, and our Indonesian collaborators, Bandung Institute of Technology, Ministry of Science and Technology, Agency for Assessment and Application of Technology, and Agency for Meteorology, Climatology, and Geophysics.

## REFERENCES

- Behrens, J., Androsov, A., Babeyko, A. Y., Harig, S., Klaschka, F., and Mentrup, L. (2010). A new multi-sensor approach to simulation assisted tsunami early warning, *Nat. Hazards Earth Syst. Sci.*, 10, 1085-1100, doi:10.5194/nhess-10-1085-2010.
- Bernard, E. N., H. O. Mofjeld, V. Titov, C. E. Synolakis, & F. I. Gonzalez. (2006). Tsunami: Scientific Frontiers, Mitigation. *Forecasting and Policy Implications. Phil. Trans. R. Soc. A. Math. Phys. Eng. Sci.* **364** (1845): 1989-2007.
- Boulos, G. Huggins, L., Siciliano, M., Yackovich, J., Ling, H., Mossé, D., Comfort, L. (2011). Detecting and communicating risk of near-shore tsunamis: Coupling near-shore sensor networks with land-based modeling for Padang, Indonesia. *Journal of Comparative Policy Analysis*. Vol. 14, 2, 1-15.
- Cabinet Office of Japan, (2011). White Paper on Disaster Management (in Japanese). Available at [http://www.bousai.go.jp/hakusho/H23\\_zenbun.pdf](http://www.bousai.go.jp/hakusho/H23_zenbun.pdf)

- Comfort, L. (2007). Crisis Management in Hindsight: Cognition, Communication, Coordination, and Control. *Public Administration Review*. Vol. 67. Special Issue, Administrative Failure in the Wake of Katrina. December. Pp. S188-S196.
- Freitag, L., M. Johnson, M. Stojanovic, D. Nagle and J. Catipovic, "Survey and analysis of underwater acoustic channels for coherent communication in the medium-frequency band," *Proc. Oceans 2000*, Providence, RI, Vol. 1, pp. 123-128, 2000.
- Lauterjung, J., Münch, U., and Rudloff, A. (2010). The challenge of installing a tsunami early warning system in the vicinity of the Sunda Arc, Indonesia, *Nat. Hazards Earth Syst. Sci.*, 10, 641-646, doi:10.5194/nhess-10-641-2010.
- McCloskey, J., Lange, D., Tilmann, F., Nalbant, S. Bell, A., Natawidjaja, D., and Rietbrock, A. (2010). *Nature Geoscience*, 3:February, 70-71.
- Meinig, C., S. E. Stalin, A. I. Nakamura, F. Gonzalez, and H. B. Milburn, 2005: Technology developments in real-time tsunami measuring, monitoring and forecasting. *Oceans 2005, MTS (Marine Technology Society)/IEEE Proceedings*, Vol. 2, IEEE, 1673–1679.
- Morrissey, W. (2005). *Tsunamis: Monitoring, Detection, and Early Warning Systems*. Washington, DC: Congressional Research Service. Order Code RL32739, 1-8.
- Paros, J.; Bernard, E.; Delaney, J.; Meinig, C.; Spillane, M.; Migliacio, P.; Tang, L.; Chadwick, W.; Schaad, T.; Stalin, S. (2011). "Breakthrough underwater technology holds promise for improved local tsunami warnings," *Underwater Technology (UT), 2011 IEEE Symposium on and 2011 Workshop on Scientific Use of Submarine Cables and Related Technologies (SSC)*, vol., no., pp.1-9, 5-8 April 2011. doi: 10.1109/UT.2011.5774145
- Satake, K., Okal, E. & Borrero, J. (2007). *Tsunami and Its Hazards in the Indian and Pacific Oceans*. Boston, MA: Springer-Verlag.
- Singh, S., Pérez -Campos, X., Iglesias, A., Melgar, D. (2012). A Method for Rapid Estimation of Moment Magnitude for Early Tsunami Warning Based on Coastal GPS Networks. *Seismological Research Letters*(May 2012), 83(3):516-530
- Strunz, G., Post, J., Zosseder, K., Wegscheider, S., Mück, M., Riedlinger, T., Mehl, H., Dech, S., Birkmann, J., Gebert, N., Harjono, H., Anwar, H. Z., Sumaryono, Khomarudin, R. M., and Muhari, A. (2011). Tsunami risk assessment in Indonesia, *Nat. Hazards Earth Syst. Sci.*, 11, 67-82, doi:10.5194/nhess-11-67-2011.
- Titov, V., Gonzalez, F., Bernard, E., Eble, M., Mofjeld, H., Newman, J. and Venturato, A. (2003). *Real-Time Tsunami Forecasting: Challenges and Solutions*. Netherlands. Kluwer Academic Publishers, pp. 1-16.
- UNESCO IOC Data Buoy Cooperation Panel, International Tsunameter Partnership. (2011). *Ocean Data Buoy Vandalism - Incidence, Impact and Responses*, DBCP Technical Document No. 41, Version 1.
- United Nations. (2005a). *Humanitarian Response Review*. New York and Geneva: Office for the Coordination of Humanitarian Affairs. August.
- United Nations Educational, Scientific and Cultural Organization. (2005b). *IOC Principles and Strategy For Capacity Building*. Intergovernmental Oceanographic Committee [IOC] General Assembly. June. [http://ngdc.noaa.gov/hazard/tsu\\_db.shtml](http://ngdc.noaa.gov/hazard/tsu_db.shtml))




---

**TSUNAMI MITIGATION PLANNING IN PACITAN, INDONESIA: A REVIEW OF EXISTING EFFORTS AND WAYS AHEAD**

**A. Muhari**

*Ministry of Marine Affairs and Fisheries (KKP), Jakarta 10110, Indonesia  
Disaster Control Research Center, Tohoku University, Sendai 980-8579, Japan*

**M. Mück**

*German Remote Sensing Data Center (DFD), German Aerospace Center (DLR), 82234 Wessling, Germany*

**S. Diposaptono**

*Ministry of Marine Affairs and Fisheries (KKP), Jakarta 10110, Indonesia*

**H. Spahn**

*GIZ International Services, Jakarta 10310, Indonesia*

**ABSTRACT**

A small bay-town in East Java Province, Indonesia is selected as a pilot area for an integrated model of tsunami mitigation. Located at the south coast of Java, Pacitan is facing a seismic gap between two tsunami-earthquake events, which are the 1994 (M 7.2) and the 2006 tsunami (M 7.7). The efforts were started in 2008 by constructing the structural components in stages. Coastal forests development and the installation of land-based ocean radar were completed within 3 years. In line with these efforts, comprehensive risk assessment is now being conducted. Detailed tsunami simulations were carried out in addition to the preparation of vulnerability analysis. We attempted to establish novel risk assessment methods and products. We complete the countermeasures by planning two-year activities of community preparedness to ensure the sustainability of the above mentioned efforts. The key objective is the development of a comprehensive and coherent tsunami mitigation system on local level.

**Keywords:** *Tsunami mitigation, Risk assessment, Numerical simulation, Decision support system, Capacity building*

# 1 INTRODUCTION

## 1.1 Background

Two mega-tsunamis hit two different countries in the last 8 years. Although punctuated by several events that are also not a small tsunami, the 2004 Indian Ocean earthquake tsunami (M 9.1) and the 2011 Japan earthquake tsunami (M 9.0) are two of the most significant events in the last 50 years. These events had two different impacts on coastal communities. Due to different disaster management conditions, the 2004 Indian Ocean tsunami killed at least 250 thousand people with 150 thousand of them in Indonesia. At that time, there were no tsunami disaster mitigation efforts, including tsunami early warning devices available (e.g. Muhari et al. 2007). In contrary, the 2011 tsunami hit a country that was equipped with one of the best tsunami mitigation and early warning systems in the world (e.g. Imamura and Abe. 2009, Shuto and Fujima. 2009). Even though still 19.000 people were missing and died as a result of the tsunami (NPA, 2012), the intervention of those structural countermeasures in line with continuous public education significantly reduced the number of casualties. On deriving the objective, this paper is advantaged by the above two tsunami experiences. We suppose that if the integrated mitigation efforts are available, the potential of human risk due to tsunami can be significantly reduced by continuously educating people in tsunami prone areas.

We are first looking back to the mile-stones reached as a response to the 2004 Indian Ocean tsunami in Indonesia. In the aftermath of the catastrophe, an ‘end-to-end’ tsunami warning system was designed and developed (Rudloff et al. 2009, Lauterjung et al. 2010). Although the system is seemed to need more time to be fully functional, it is already able to issue the warning within 5 min (Pariatmono. 2012). The dissemination process seems to be the priority problem to enhance in the near future. Hayden et al. (2007) said that the role of warning dissemination is a key part in the success of such large-scale evacuations and its inadequacy in certain cases has been a ‘primary contribution to deaths and injuries.’ Experiences in the case of the 2010 Mentawai Islands tsunami-earthquake where the tsunami arrival time was less than 15 min (Muhari et al. 2010), and the 2011 Japan tsunami in Papua region where the tsunami was lasting up to 12 hours (Khafid and Handayani. 2011) are still the main weaknesses of the present system on disseminating and terminating the warning. As locals in Mentawai Island could not obtain fast warning due to insufficient warning time during the 2010 tsunami-earthquake, it yield to 546 casualties as a result of late evacuation. In Papua region, the long wave propagation passing through ocean ridges created several wave trains due to the trapped tsunami energy and excites ridge waves during the 2011 Japan tsunami (Koshimura et al. 2001). However, tsunami warning was terminated after the second wave in the first wave train (Fig 1). As the result, a locality returns to the lowland area and was swept by the next waves.

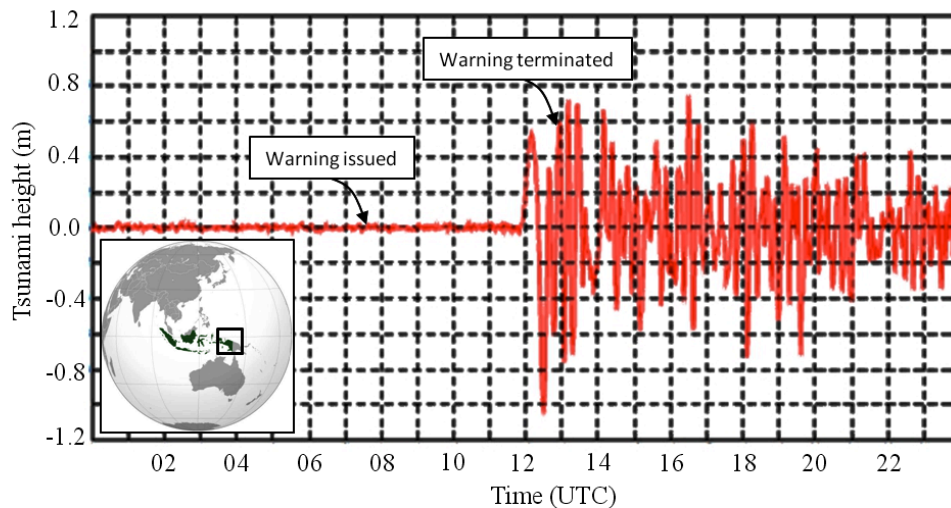


Fig 1: The tide gauge record in Jayapura, Papua, Indonesia during the 2011 Japan tsunami

The next problem is the inappropriate response of people to the tsunami warning and limited structural facilities to reduce tsunami impact and evacuation measures. Results of the questionnaire survey after the doublet outer-rise earthquake in April 2012 off the Simelue Island, Indonesia stated that even people in Banda Aceh are still have inadequate behavior to respond adequately to the warning and to start the evacuation (I-RAPID. 2012 and J-RAPID. 2012). For the latter, such situations do not only occur in areas with limited experience with tsunamis. In Japan, the inappropriate behavior especially during evacuation such as using cars, 'family evacuation' and underestimating the hazard that yields to the delay of evacuation was repeatedly observed. In this case, sustainable education might be the only solution. Dengler (2004) said that tsunami education activities have been proven as the essential tools for near-source tsunami mitigation. This might be correct especially for the children. A success story of an amazing evacuation conducted by students of an Unosumai Elementary School in Kamaishi Town, Japan is one of the warrants that continuous education can bring significant change on how people respond to the tsunami warning (e.g. Katada, 2011).

Learning from the above-mentioned experiences and literature, we design comprehensive countermeasures to be implemented in a pilot area in Indonesia. Pacitan, a small bay-town in the south of Java, Indonesia is selected as a case study. A step-by-step planning is consisting of three main parts of activities: the first is the tsunami hazard-vulnerability and risk assessment, followed by the development of structural countermeasures, and finally, the most important process to ensure the sustainability of the above efforts, the capacity development concept on tsunami preparedness, awareness and close assistantship in public education programs. This paper is aimed to described the concept and explain the past and ongoing processes in Pacitan town and district. The explanations are complemented by the future planned activities in the next two years in the framework of a research cooperation and project between Indonesia (KKP) and Germany (PROTECTS project).

## 1.2 Overview of the pilot area

Pacitan lies on  $8^{\circ} 11' S$  and  $111^{\circ} 7' E$ . The U-shape bay regency is facing the southern part of the Indian Ocean and is characterized by flat topographic conditions with average ground level of 4 to 5 m. Historical earthquakes compiled by Newcomb and McCann (1987) in Fig. 2 indicate that there were no significant large earthquake occurred in the last 150 years. However, it should be noted that even the earthquakes were not so strong; three last earthquakes on that region generated significant tsunamis along the coast. In the easternmost part of the region, the 1977 outer-rise earthquake ( $M 8.3$ ) occurred with a maximum run-up of 8 m in Lunyuk, Sumbawa Island (Gusman et al. 2009). In 1994, either tsunami earthquake (Polet and Kanamori, 2000) or slip over subducting seamount (Abercrombie et al. 2001) with  $M 7.6$  generated a maximum of 14 m tsunami in Banyuwangi, East Java Indonesia (Tsuji et al. 1995). In the westernmost part, a  $M 7.8$  earthquake generated an extreme run-up height of 21 m in West Java, Indonesia (Fritz et al. 2007). The very long seismic signal and significant discrepancy between the earthquake magnitude and the resulting tsunami height suggested that this event is a tsunami-earthquake (e.g. Ammon et al. 2006). Among the 1994 and the 2006 events, there exists a seismic gap that is directly facing Pacitan town (Fig. 2). We assume that the gap will be the source for future tsunamis particularly for Pacitan town, thus the hazard analysis will focus to explore the potential impact due to the tsunami generated in the existing gap.

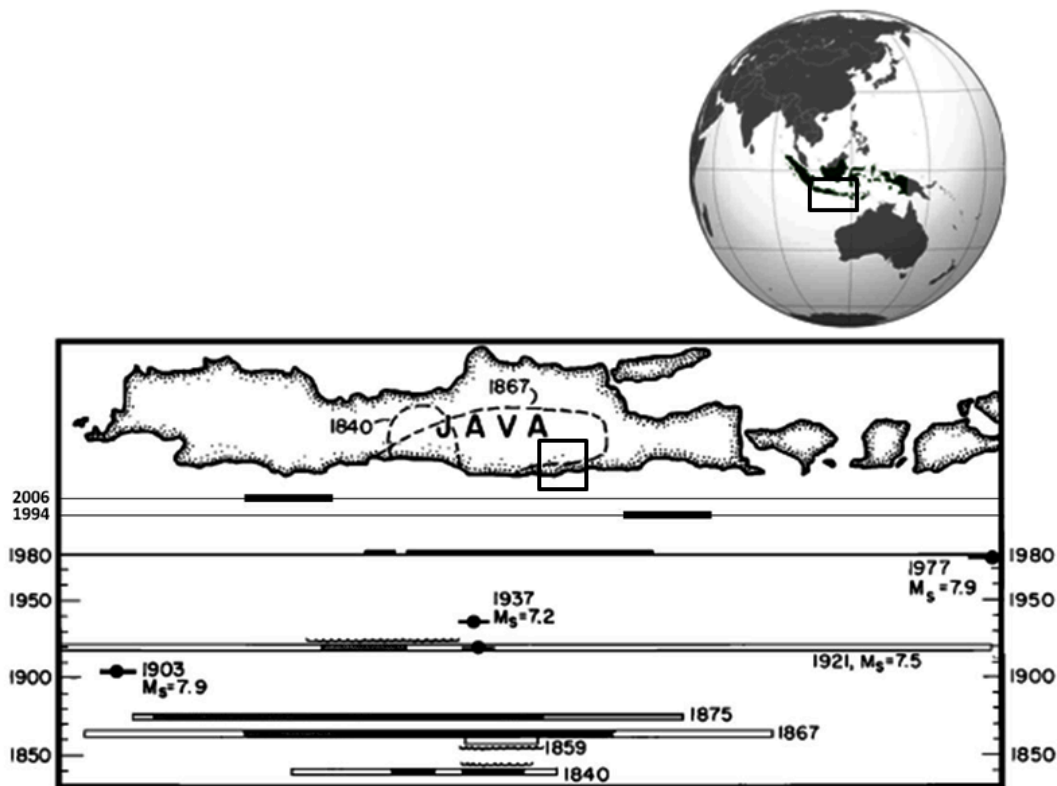


Fig. 2: Historical earthquake along the south part of Java Island (inset is the location of Pacitan)

### **1.3 Outline of the paper**

This paper is first describing the background of seismic hazard in Pacitan that underlies the objective of the research. Next, we formulate the concept of tsunami mitigation from a general point of view into a site specific context based on the related physical and socio-cultural aspects in Pacitan Town. The detailed tsunami hazard assessment is then carried out to evaluate the potential impact on the coastal community. Based on this information, two structural countermeasures will be described. One is the coastal forest plantation, and the second is the installation of land-based ocean radar which was finished last year. In the last part, we draw the plan for future activities based on the concept derived in the second part. Methods on vulnerability and risk assessment will be presented and key approaches for the future activities are described. Central is the development of a capacity-development concept on tsunami preparedness for local communities.

## **2 CONCEPTION OF TSUNAMI MITIGATION**

### **2.1 State of the art**

In general, mitigation is defined as any sustained effort undertaken to reduce a hazard risk through the reduction of the likelihood and/or the consequence component of that hazard's risk (Coppola 2007). It consists of two major types that are the structural and nonstructural part. It attempts to reduce the risk likelihood and risk consequences, to avoid the risk, to accept the risk and to transfer the risk.

In Japan, this concept is known as tsunami countermeasure instead of mitigation (see Shuto and Kojima. 2009). Based on 10 recommendations derived by the Council of Earthquake Disaster Prevention (CEDP) in 1933, both structural and nonstructural measures were compiled as the main effort to reduce the tsunami risk without taking into account the tsunami early warning –which was not available during that time– and the further education program. Along with the time, this concept is enhanced by the establishment of numerical models on tsunami computation that is the basic for tsunami warning systems. Also, the importance of appropriate response by the society is realized as one of the key factors for successful evacuation (e.g. Imamura 2005). Thus, the continuous assistantship and public education are necessary to reduce the risk bias (Imamura. 2009). Even though the 2011 event shows that these efforts have not shown positive results for the elderly, but it successfully suppresses the number of death among children as shown by the death distribution according to age and gender (NPA, 2011).

In the US, through the National Tsunami Hazard Mitigation Program (NTHMP), five recommendations were addressed to be conducted 4 years after the 1992 California earthquake and tsunami. The recommendations cover broader aspects such as producing inundation maps, improving seismic networks, tsunami buoys, developing hazard mitigation programs and the development of technical guidelines and supports (Bernard. 2001). The overall accomplishment and impacts of the NTHMP program on developing the resilient community is given by Bernard (2005) and Trisler et al. (2005) that indicates the significant increment of planning and coordination, information and public education feedback from 16 local emergency managers along the west coasts of the US.

In Indonesia, such an integrated concept is not yet available. The efforts are still limited on the development of the tsunami warning system (Lauterjung et al. 2010, Münch et al. 2011), while the public education and preparedness (e.g. KOGAMI. 2011, Rafliana 2012) is conducted as a not fully integrated way with the above system. As a result, response of people to conduct appropriate evacuation is still far from the appropriate condition as shown by questionnaire surveys after the last major earthquakes in West Sumatran coast in 2012 (M 8.6 and 8.0) documented by I-RAPID (2012) and J-RAPID (2012).

## 2.2 Formulation of mitigation concept in Pacitan Town

Pacitan is one of the participating districts in the “Project for Training, Education and Consulting of Tsunami Early Warning System” (PROTECTS), the follow-up project of the German Indonesian Cooperation on Tsunami Early Warning System (GITEWS), to support Indonesia in strengthening the capacity of local governments and civil society actors so as to provide the services necessary for sustainable tsunami preparedness.

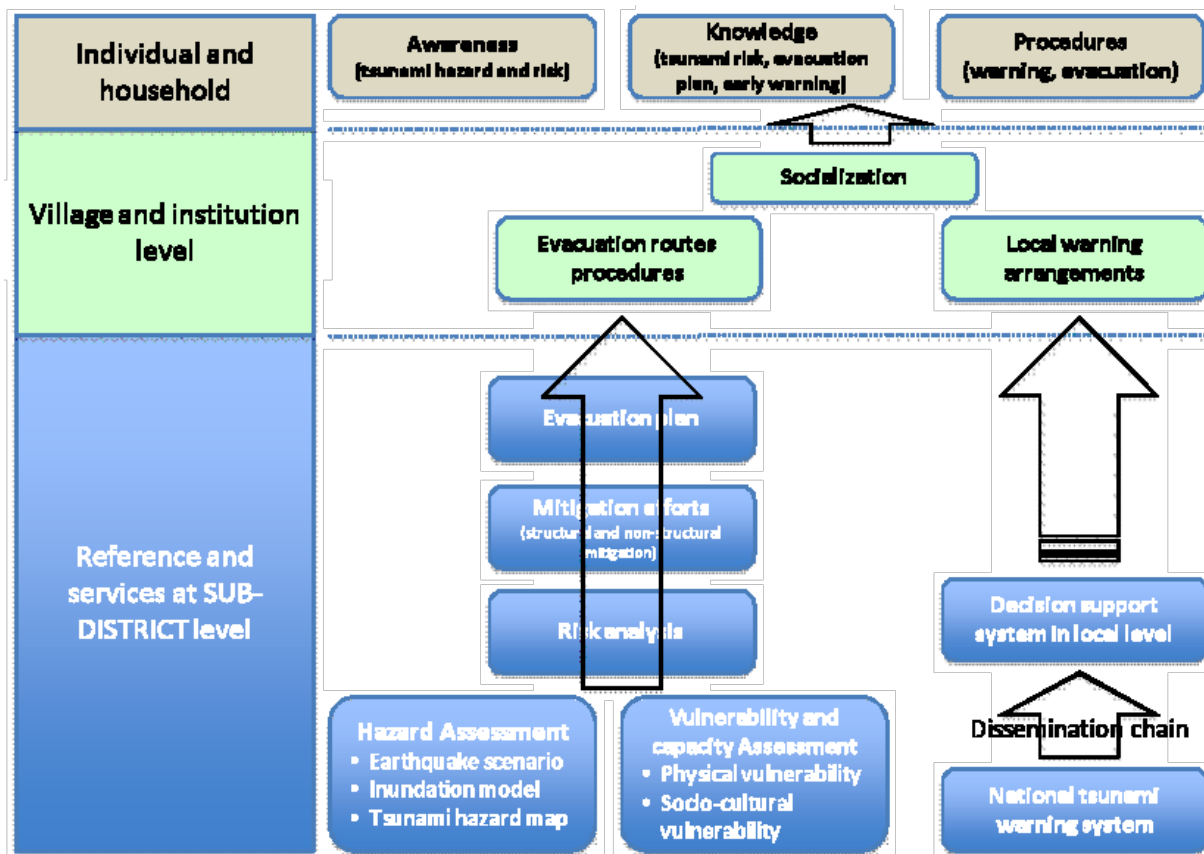


Fig. 3: Multi-level approach to strengthen tsunami preparedness (modified from GIZ-IS, 2011)

Within the agreed tsunami mitigation concept focussed on the capacity-development for local communities, which was designed by the German Agency for International Cooperation (GIZ) together with the Indonesian National Board for Disaster Management (BNPB), and a number of provincial disaster management agencies (BPBD), a multi-level approach involving key players at all levels is implemented since June 2011. It follows a step-by-step approach as described in Fig. 3 to build awareness, knowledge and solid procedures within at-risk communities.

This approach addresses the specific conditions in the context of near-field tsunamis (short arrival-times, high level of uncertainty) which require that individuals are enabled to quickly take decisions and correct actions even in the absence of guidance from local authorities or the failure of warning services during an emergency. Local evacuation maps and procedures and warning arrangements are needed to support people in the risk areas in this regard. To develop such plans at village level it requires references regarding hazardous and safe zones and recommended evacuation strategies, as well as the development of local warning services. The responsibility to provide such references, including risk assessments, evacuation plans and the setting up of mechanisms for decision-making and warning dissemination to the community at risk lies with district government. Consequently, the capacity building approach starts by addressing the district level, especially the local disaster-management agencies, first.

The capacity-development process is facilitated through a sequence of workshops, implemented by the provincial government, involving representatives from local working groups. During the workshops the participants are introduced to the main topics, such as hazard and risk assessments, evacuation planning, the local warning chain, community awareness and tsunami-simulation exercises. Between the individual workshops the local working groups are in charge to implement the required action in their respective areas. The project offers technical trainings on evacuation planning and local warning services as well as preparing local facilitators to support preparedness processes at village level and to implement community awareness campaigns at grass root level.

Beside the implementation of a capacity-development concept on tsunami preparedness, a good and complete understanding of the overall set up of the Indonesian Tsunami Early Warning System (InaTEWS), the time line, the warning scheme and how warnings are being distributed is needed by all actors who are involved in the development of the local warning dissemination mechanism. The National Agency of Meteorology, Climatology and Geophysics (BMKG) operates the National Tsunami Warning Center (NTWC) in Indonesia and is the only appointed official institution responsible to generate tsunami warnings. Using multiple communication channels, BMKG produces and sends tsunami warnings from its Warning Center in Jakarta to 'Interface Institutions (media, local governments, emergency operation centers, etc.). Local authorities in tsunami-prone areas are in charge of informing their communities about an imminent threat and providing clear guidance on how to react. Near-field tsunamis, however, give only little time for warning and evacuation, so local dissemination must be quick and reliable (GIZ, 2010c). However, the uncertainty on the hazard posed by tsunami sometime cannot be judged by the limited equipment of the national tsunami warning. For instance, during the 2011 tsunami, the tsunami warning in Japan (that is claimed as the best system in the world) predicts only M 7.9 after the massive earthquake with (actually) M 9.0-9.1. The JMA

issued tsunami warning of 3 m tsunami height in Iwate and 6 m in Miyagi. But the actual tsunami observed by the GPS buoys informs that tsunami have been formed with 7 m height in front of Iwate coast (MLIT, 2011). In this sense, the availability of multi-layer equipment for near-field tsunami warning is subsequently necessary to update the first prediction made by the tsunami simulation data base. In Pacitan, therefore, we designed a decision support system for the local government (towns or city level) using a High Frequency (HF) radar antenna to observed continuously the current properties of the ocean. Even though the use of ocean radar in tsunami warning is still in development (Borner et al. 2010, Gurgel et al. 2011, we attempt to prepare the equipment we need on developing the technology. During the planning of the local decision support system, we plant and construct coastal forest along the east part of Pacitan Bay. Shuto et al (1985) said the coastal forest only effective to reduce tsunami with a height less than 3 m. However, their configuration along the coast could be useful on reducing the number of floating debris carried out by the tsunami inland.

The subsequent phases of the concept displayed in Fig.3 will be explained in the following.

### 3 THE PAST AND ONGOING ACTIVITIES

#### 3.1 Tsunami hazard assessment

We determine the source scenario as parametric study using four hypothetical sources. Four scenarios are selected to cover the earthquake magnitude ranges from 7.5 Mw – 8.5 Mw. In the biggest magnitude, we add another scenario that accommodates the potential of slip in updip near the trench as given in Table 1. We assumed the strike, dip and rake as 284°, 12° and 99°. Particularly for the tsunami-earthquake component, we assumed that the additional slip in shallow sediment has the dip of 60°. This is the same value of additional slip as for the 1994 tsunami in East Java proposed by Latief (2000). Also, for all fault parameter, we assumed homogenous rigidity as  $3.5 \times 10^{10}$  N/m<sup>2</sup>.

Table1. Hypothetical sources used for the numerical model

No	Length	Width	Mw	Depth	Rake	Dip	Strike	Slip
1	80000	40000	7.5	10	99	12	284	2.50
2	150000	70000	8	10	99	12	284	4.00
3	300000	150000	8.5	10	99	12	284	4.57
4	200000	100000	8.5	10	99	12	284	4.50
	200000	10000		1.4	99	60	284	4.50

The epicenter of the earthquake is assumed in the middle of the largest rupture area (arrow in Fig. 4). We numerically computed the above source scenarios using half space method proposed by Okada (1985).

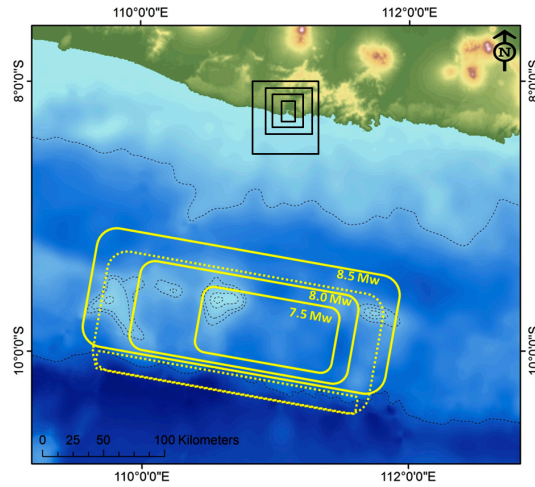


Fig 4. Rupture areas of the hypothetical sources. Dashed lines show the tsunami-earthquake scenarios, inset box are the nested region for inundation model in Pacitan Town. Concurrently from the largest to smallest are the regions 1 to 5.

The initial tsunamis are then propagated numerically using shallow water equation and discretized using the finite different method in a leap frog scheme given by Imamura (1996). We divided the numerical domain into five regions. Region 1 using numerical grid size of 648 m resampled from GEBCO\_08 data (British Oceanographic Data Center, 2008) with original accuracy of 30 arc-sec (about 926m) with using the nearest neighbor method. Region II and III are obtained from the similar data set resampling method to create 162 m cell size for region II and 40.5 for region III. For region IV and V, we used SRTM best tile (DLR, 2009) with accuracy of 30 m. However, one should note that topographic data in SRTM used in this research is the ‘surface elevation’ data that consists of all nature and man-made structures. Ideally, the SRTM data should be manually corrected with the average height of land cover features like it was demonstrated by Roemer et al. (2012), but the lack of field survey data made it impossible to determine the average height of the land-cover features. Thus, such a limitation is highly acknowledged that it may reduce the accuracy of the resulting numerical calculation on tsunami inundation. The SRTM best tile data is resampled into 13.5 m for region IV and 5 m for region V. We manually digitized the local nautical chart for Pacitan waters obtained from the Indonesia Navy No. 70, and manually smoothes the chart in the coastal area.

The set of equations used in the numerical model is given as follow,

$$\frac{\partial \eta}{\partial t} + \frac{\partial M}{\partial x} + \frac{\partial N}{\partial y} = 0 \tag{1}$$

$$\frac{\partial M}{\partial t} + \frac{\partial}{\partial x} \left[ \frac{M^2}{D} \right] + \frac{\partial}{\partial y} \left[ \frac{MN}{D} \right] + gD \frac{\partial \eta}{\partial x} + \frac{gn^2}{D^{7/3}} M \sqrt{M^2 + N^2} = 0 \tag{2}$$

$$\frac{\partial N}{\partial t} + \frac{\partial}{\partial x} \left[ \frac{MN}{D} \right] + \frac{\partial}{\partial y} \left[ \frac{N^2}{D} \right] + gD \frac{\partial \eta}{\partial y} + \frac{gn^2}{D^{7/3}} N \sqrt{M^2 + N^2} = 0 \quad (3)$$

$$M = \int_{-h}^{\eta} u \, dz, \quad N = \int_{-h}^{\eta} v \, dz, \quad D = h + \eta \quad (4)$$

In these equations,  $M$  and  $N$  denote the discharge flux in the  $x$  and  $y$  directions, respectively;  $\eta$  denotes the water elevation,  $n$  stands for the Manning coefficient, and  $h$  represents the water depth.

In the case of run-up, the friction component should accommodate different roughness values due to different land cover. Here, we used a method of Equivalent Roughness Model (ERM) by taking into account the resistance due to different roughness values in non-residential areas, and combining different roughness and drag force due to the existence of buildings in residential areas. The formulation derived by Aburaya and Imamura (2002) is given below, while detailed explanation on its implementation in densely populated area given by Muhari et al. (2011).

$$n_e = \sqrt{n_0^2 + \frac{C_D}{2gk} \times \frac{\theta}{100 - \theta} \times D^{4/3}} \quad (5)$$

Here  $n_e$  is the equivalent roughness,  $n_0$  is the original Manning coefficient where variation depends on the land cover.  $\theta$  is the percentage of the bottom area occupied by the building in a grid on the numerical domain and  $D$  is the flow depth.  $C_D$  is the drag coefficient. FEMA 55 (FEMA, 2003) suggests drag coefficient values from 1.25 to 2, depending on the ratio between the width of building and the flow depth. In case of highly populated areas where the building size varies from small to large, it will be very difficult to assign different values for each building. Therefore, in this case, we choose a fixed average value as 1.5 applied in the residential area.

By using the above equations, the initial sources is numerically propagated and inundated for 3 hours simulation with 0.25 sec time step. The snapshot of tsunami propagation (in case of the tsunami-earthquake) is given by Fig. 5.

Impressions from the above snapshot files are that the existence ridges waves when tsunami passes through the sea mount just after it propagates 5 min from the source. Even though the strike of the source was made to be parallel to the coastline –in order to maximize the tsunami impact–, the above mention phenomenon showing the energy radiation is not directly hitting Pacitan Town as visualized in Fig. 6.

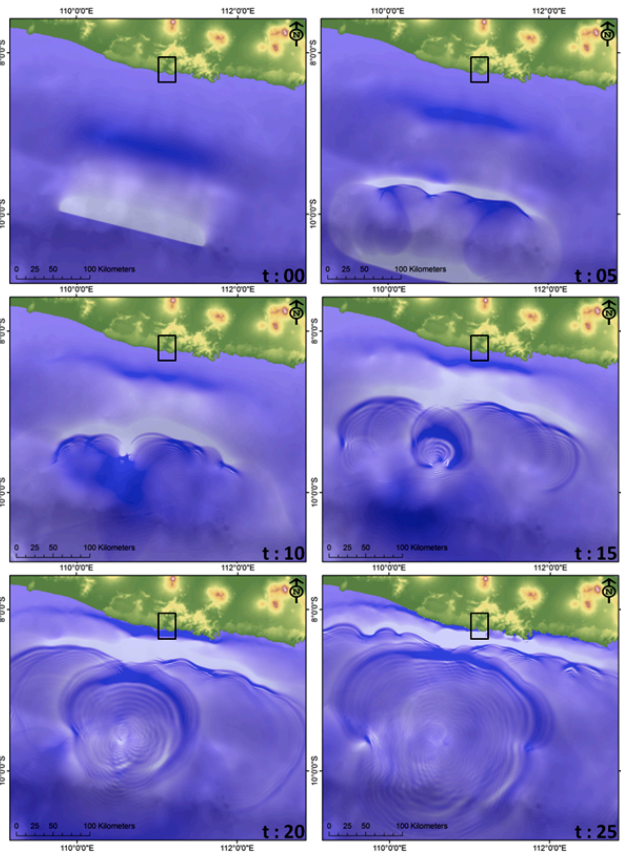


Fig.5: Snapshot of tsunami propagation from the tsunami-earthquake scenario

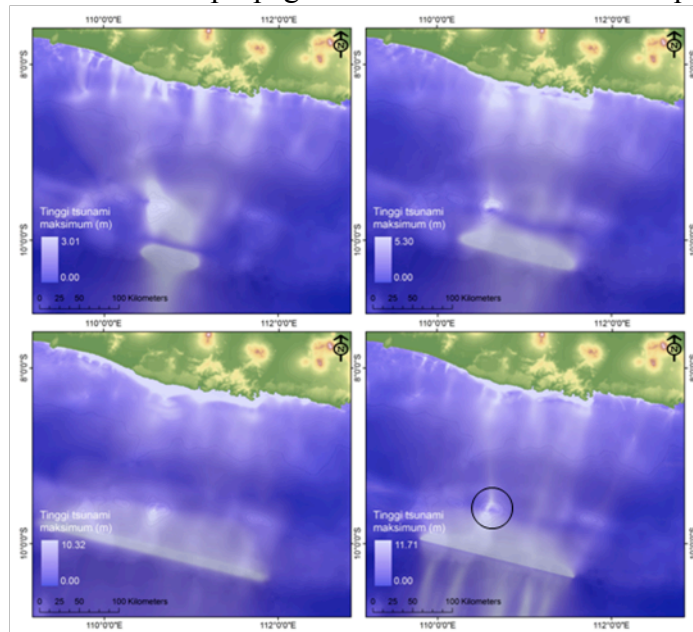


Fig.6. Distribution of maximum tsunami height from each scenario

The result of numerical simulation suggests that the scenario 4 produced the worst impact in term of the maximum tsunami height along the coast. Thus, it used for further analysis to assess the inundation pattern. We prepared the input data for inundation model as given in Fig. 7. Beside the topographic data (Fig. 7, left), a land use file was put in a separate file to calculate the roughness except building/houses (Fig. 7, center). For residential areas, another file consisting of the percentage of building occupancy on each numerical grid is prepared also in a separate file (Fig. 7, right). These data will be used simultaneously during the calculation.

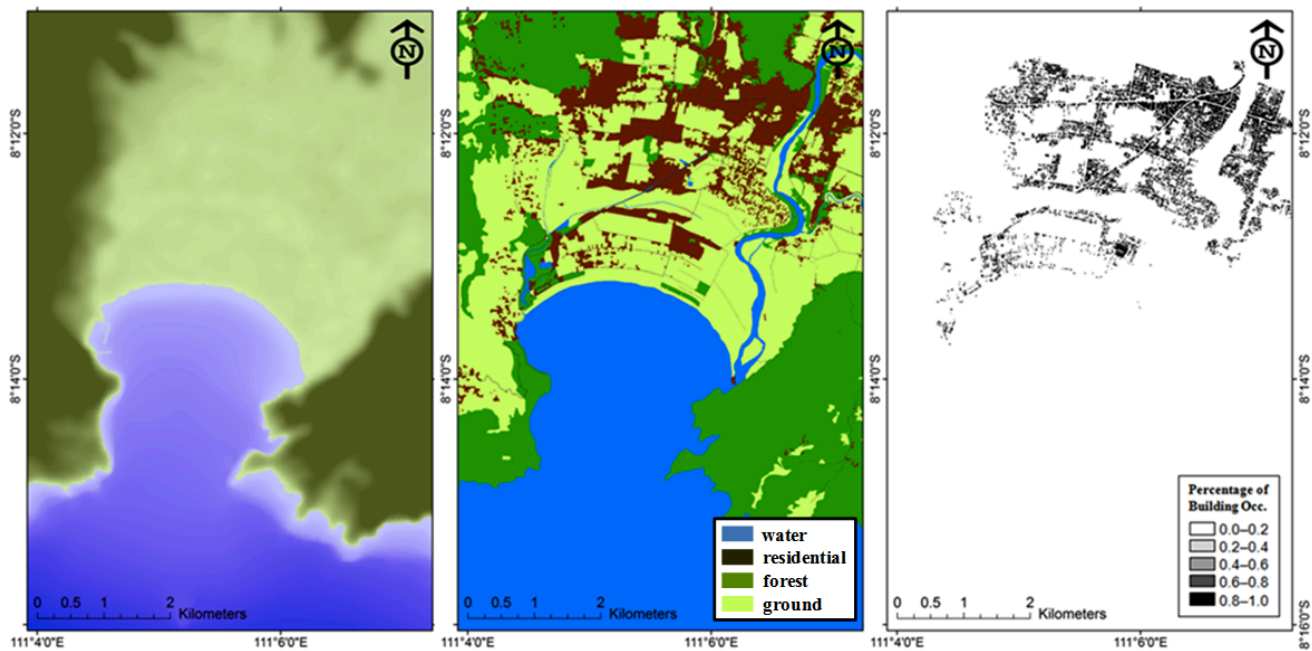


Fig.7. The input data for calculation of tsunami inundation: topographic data (left), land use data (center) and percentage of building occupancy (right).

The values of Manning roughness for specific land use is referred to Kotani et al. (1997). We visualized the results of the inundation model in Fig.9. It can be seen that a tsunami is potentially flooding Pacitan Town with a maximum flow depth of 10.8 m and in average of 4 m. The area on the right hand side of the bay (right side of the river) is the lowest ground level in the numerical domain. Hence, the area shows the deepest flow depth in the region. The flow velocity is modeled with a maximum of 14.59 m/sec inside the fishery port (in the left part inside the harbor) and an average of 3.6 m/sec.

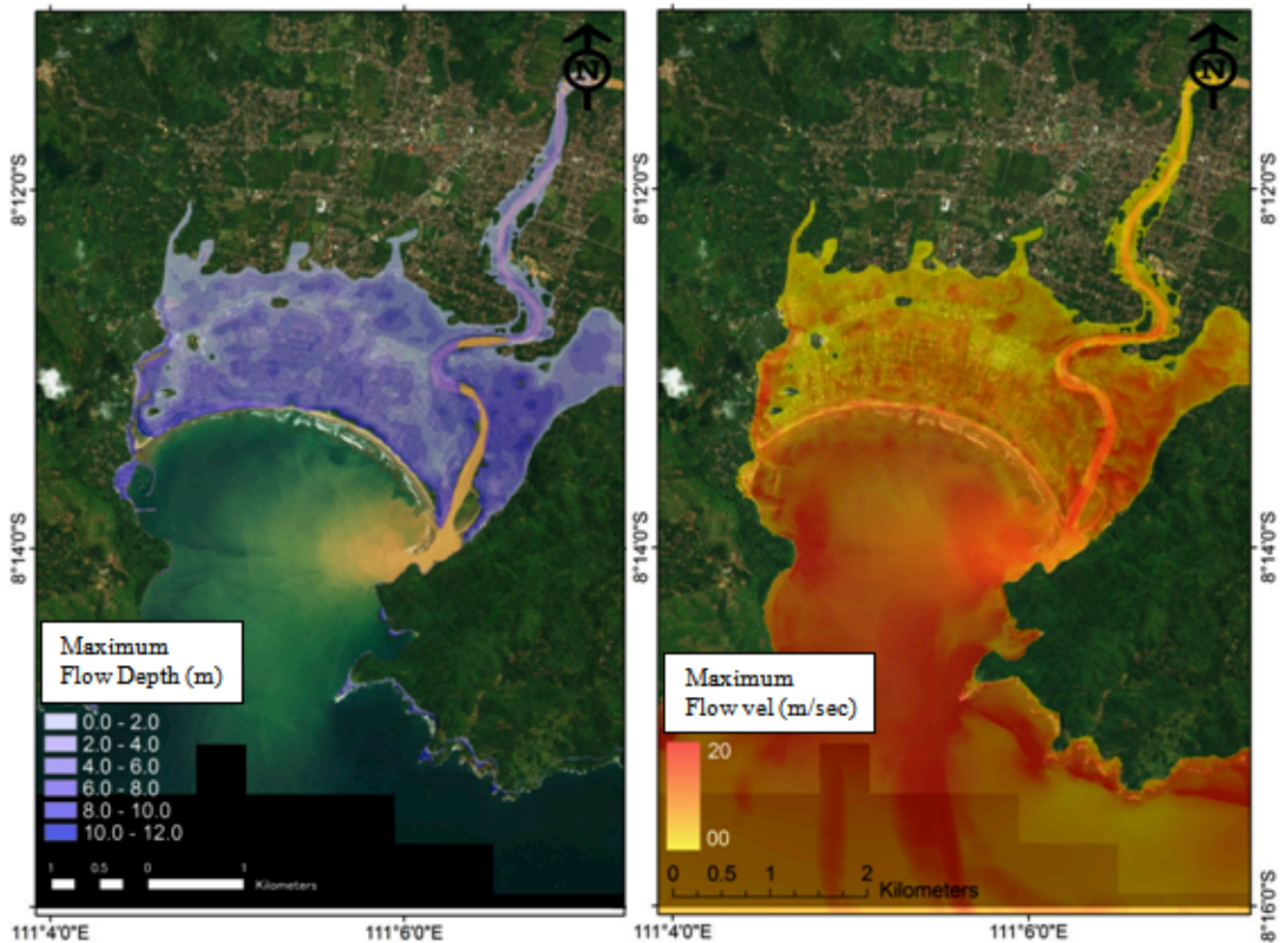


Fig.9. Distribution of maximum tsunami flow depth and flow velocity

### 3.2 Coastal forest plantation

The coastal forest was planted in 2 phases, first was started in 2008 and the following phases was conducted in 2011 (Fig. 10). We use whistling pine (*Casuarina equisetifolia*) that has been proven to be appropriate for the sand type beach in south Java coasts (MoMAF, 2011). Previously, Shuto (1993) said that coastal forest can be functioned to stop the floating debris if the tsunami height less than 3 m. Furthermore, Harada and Imamura (2005) stated that the reduction of the tsunami inundation extent, flow depth, flow velocity and hydrodynamic force will be depending on the width and density of the trees in the forest. They conclude that a 200 width of coastal forest might be able to reduce the inundation extent and flow depth of a 3 m tsunami up to 80%. Also, it can be very useful to reduce tsunami energy of a 3 m tsunami up to 30%.



Figure 10. Location of the coastal forest development in Pacitan Bay

We plan to construct at least 100 m width of coastal forest. In the first and second step, the built coastal forest has 70 m width. Actually, original land that has been used is around 100 m. However, the trees that were planted in the back of the present coastal forest (Fig. 11) was the different type of whistling pine. It was planted by –locally called– ketapang (*Terminalia Catappa*). Unfortunately, this species is not successfully growth so it left an empty space behind the present forest. The problem why the second species is not growth is still left for further analysis.



Figure 11. Planting and the growth of whistling pine in Pacitan Bay

### 3.3 Local decision support system

The first local decision support system for tsunami warning in Indonesia is introduced by Muhari et al. (2010) using tide gauges. They put a tide gauge in a small island around 11 km from the city, and in real time the data was transferred to the base station in emergency office using radio frequency. However, not all tsunami prone cities in Indonesia has small island in front of them that can be used to install the tide gauge. Pacitan Bay is one of them. Therefore, we are looking for another alternative to develop the system that can help the local authorities to make an appropriate decision once the big earthquake occurred. The selection to choose radar system was motivated by facts that it can detect the 2011 Tohoku tsunami in Chili and Japan (Lipa et al. 2011). However, it has been admitted that up to present, the radar equipment is able to detect tsunami after it confirmed by the other data (such as tide gauge). There is no such a function that automatically discriminate which is tsunami and which is not available from the radar in the present time. Therefore, the development of automatic algorithm for the radar to detect the tsunami is still being intensively discussed. We believed, with the ability to detect the ocean current up to 150 km offshore, this equipment could become the basis for the decision support system or even the local tsunami warning in the future. To date, we already install the radar sensor and the visualization of the data was interfaced in Indonesian as given in Fig. 12.

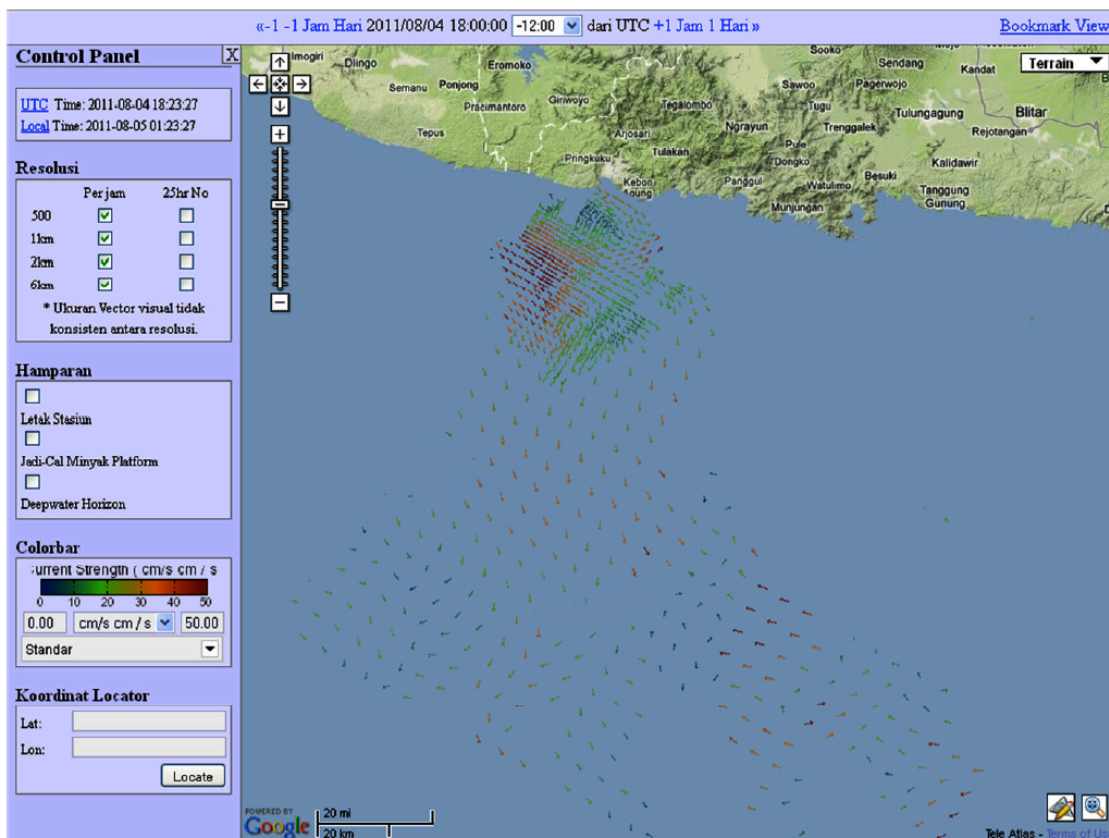


Figure 12. Visualization of the radar data in a simple interface

## 4 FUTURE PLANNED ACTIVITIES

As shown in Fig.3, risk information is a crucial precondition for the implementation of tsunami preparedness strategies for local communities. Risk knowledge within this framework specifically refers to the knowledge of probabilities of hazard distribution on land and the question whether elements are exposed to the hazard. For the case of tsunami the knowledge of the area inundated by tsunami is necessary for defining the evacuation zone and the deployment of warning dissemination infrastructure, such as sirens. But risk knowledge is not limited to hazard and exposure assessment. As already defined, vulnerability assessment refers to analyzing the underlying factors that determines the likelihood of damage and loss of life during and after an extreme event.

Within the PROTECTS project, the German Aerospace Center (DLR) is responsible to provide risk information for the participating districts as a basis for further capacity development and evacuation planning. Available hazard assessment results (see 3.1) are the basis for the development of 3 map products for Pacitan district covering vulnerability and risk information. The method developed within the GITEWS project (Strunz et al., 2011) will be used as explained in the following subsections.

### 4.1 Exposure map

In case of a tsunami, the decision whether a region should be warned requires sound information on the spatial distribution of exposed population in order to prioritize tsunami warnings and to develop efficient evacuation planning strategies. In Indonesia, population distribution data are available for villages as smallest administrative level provided by the National Statistical Agency (BPS). To improve the spatial resolution of population data, a method to disaggregate population information from available datasets to land use classes was developed and validated by Khomarudin et al., (2010) as shown in Fig.13,

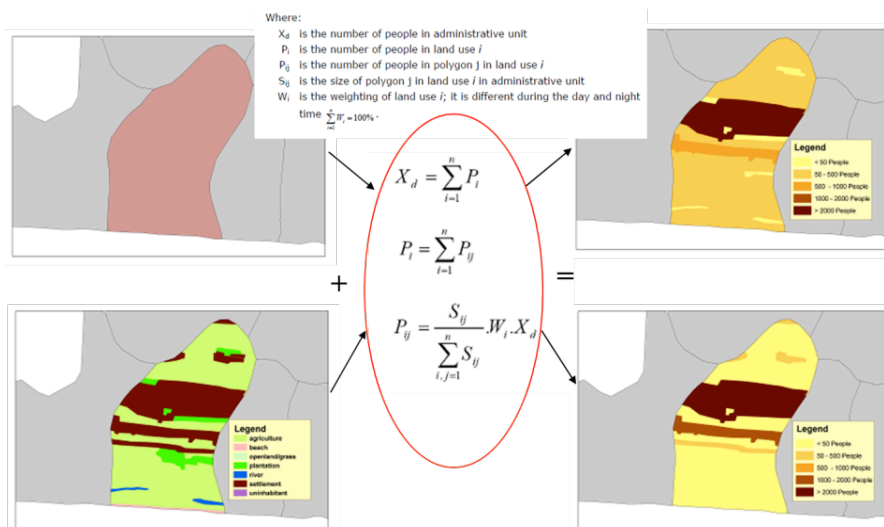


Fig.13. Concept of population distribution modeling

Here, statistical analysis of people's activities is used to allocate weights for the disaggregation whereby the determination of weighting factors that distribute the population to land use classes during day- and night-time is crucial. There are two sources of statistical data in Indonesia that provide information. Site specific information on the livelihood of population is necessary to apply this method in order to calculate the potential number of people engaged in different land use activities at various times of the day. The result of the population distribution modeling, finalized within this project, will be an enhanced population density map (day and night distribution) for Pacitan town with a scale of 1:25 000.

## 4.2 Evacuation time map

Having the information of tsunami hazard and the potential exposed people, we will start to develop the evacuation plan. In this step, the concept of evacuation time map (Post et al. 2009, Wegscheider et al. 2011) will be used to spatially determine the time needed to evacuate toward specific destination inside or outside the tsunami affected areas. The conception displayed in Fig.14, briefly described that the evacuation time that influences the normal walking speed of human depends on: (1) location of tsunami safe areas and their properties, (2) land cover, (3) topography (slope), (4) population density, (5) age and gender distribution and (6) density of critical facilities (e.g. primary schools, hospitals). The location of safe areas determines the distance an evacuee has to cover. Land cover and slope alters the evacuee's movement and speed (ADPC, 2007). Related to demographic factors it has been found in several studies that age and gender distributions significantly impact fatality rates due to contributions to longer evacuation times. In evacuation modeling studies, the impact of population density and evacuation properties of different group sizes are accounted for. The larger the group and the higher the population density the slower the evacuation process (Klöpffel, 2003). The existence of critical facilities such as schools and hospitals result in reduced response capabilities due to the presence of people needing special attention during an evacuation (Johnson, 2006). Obviously physical and mental disabilities are limiting factors for individuals to cope during a disaster.

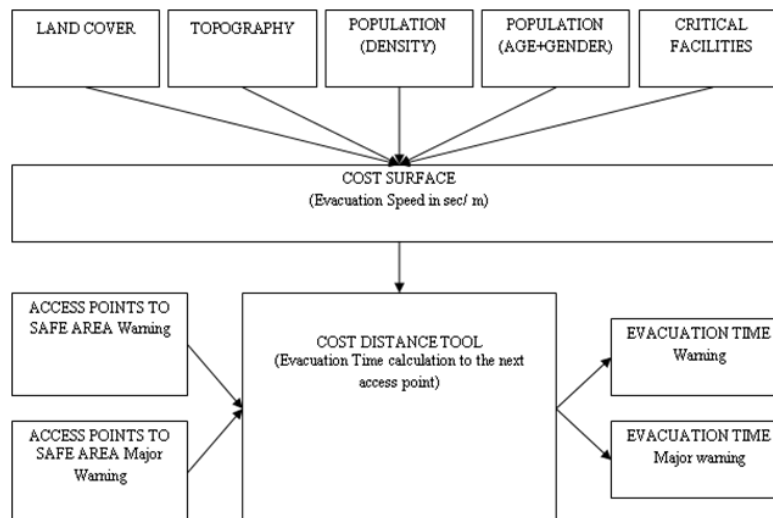


Fig.14. Concept for evacuation time modeling

The basic principle for the quantification of evacuation time is a GIS analysis to define the fastest path (best evacuation route) from a given point to the nearest safe area. Using the determined credible evacuation area, so called access points to safe areas can be assigned. Additionally, first characteristics of a safe area referred as temporary shelter areas for evacuation are determined (e.g. land cover, size, slope).

A measure of travel costs is used which can be considered as travel time (evacuation time) needed when approaching the next safe area. In this concept, the accessibility to a safe area is calculated on a cost surface which consists of a regular two dimensional grid where each cell value represents the cost to travel through it depending on costs introduced by land cover, population density, slope, critical facility density, age and gender distribution. Using the cost weighted distance approach the time needed from each location (raster cell) within the credible evacuation area to the next safe area is calculated using the ArcGIS cost distance algorithm (ESRI, 2001). For Pacitan town, an evacuation time map with a scale of 1 : 25 000 will be produced showing areas where evacuation is/ is not possible within a certain time due to available capacity of evacuation buildings (if known) and the available evacuation time (based on numerical modelling).

### **4.3 Risk map**

As risk is conventionally expressed by the equation  $\text{Risk} = \text{Hazard} \times \text{Vulnerability}$ , risk assessment is a logical outcome of the hazard and vulnerability assessment. Main objectives of the risk assessment were the identification of areas of high tsunami risk in terms of potential loss of life. Where high risk areas are identified, there is an urgent need for action by local authorities to improve the response capability of the population, thus reducing the risk. The identification of high risk areas raises the awareness of vulnerable “hotspots” and provides information vital to the support of emergency decision making. The official activities of planning and implementing risk reduction measures, like the construction of tsunami shelters, the governance of construction activities, the signposting of evacuation routes, or the installation of structural and natural coastal protection measures, need to be prioritized. The degree of risk is determined by a decision tree method as detailed explained in Wegscheider et al., (2011).

### **4.4 Evacuation planning and socialization processes**

Evacuation of people in risk areas is the first priority once a tsunami early warning is received and/or natural warning signs indicate the possibility of a tsunami. As the available time span between a warning and the impact of tsunami waves in Indonesia is generally very short, all necessary preparations need to be made in advance to ensure that as many people as possible get a chance to evacuate (Spahn et al., 2010). A five-step method for tsunami evacuation planning (Fig.15) was developed by GIZ-IS (GIZ-IS, 2010a) within the GITEWS project, enabling local authorities and other stakeholders in Indonesian communities to design, disseminate, test and improve tsunami evacuation plans. The approach will be implemented in Pacitan district for the next two years.

The planning steps →	Topics to be discussed →	Output ↓
<b>Step 1: Prepare for the planning</b>	Mandates, planning team and resource persons, data and information, resources, planning process and timeframe	Work plan
<b>Step 2: Understand your community's tsunami risk</b>	<b>Hazard:</b> inundation area and arrival time <b>Vulnerability:</b> physical exposure of population and facilities, capability to evacuate, preparedness and readiness to evacuate, early warning system Potential evacuation routes and shelter, high risk areas	Maps, data inventory, mind map and assessment report
<b>Step 3: Design your evacuation strategy and map</b>	<b>Evacuation strategy:</b> evacuation time, evacuation zone(s), safe areas, assembly areas, modes of evacuation, evacuation shelter buildings, evacuation routes, when to (self-)evacuate <b>Support during evacuation:</b> traffic management, vulnerable facilities, evacuation signage	Preliminary evacuation plan: document that include map, strategy and recommendations; draft public evacuation map
<b>Step 4: Assess, endorse and disseminate your evacuation plan</b>	Public assessment of the plan, endorsement by local authorities, dissemination to institution and public, outreach strategy	Endorsed evacuation plan, dissemination and outreach plan
<b>Step 5: Test, evaluate and improve your evacuation plan</b>	Tsunami simulation exercises, means of observation and evaluation, revision of evacuation plan	Plan to test, evaluate and improve the evacuation plan

Fig.15. Five-step concept for tsunami evacuation planning (GIZ-IS, 2010a)

## 5 CONCLUSIONS

We reported past, ongoing and future activities on developing an integrated tsunami mitigation in Pacitan Town, Indonesia. Started with the tsunami hazard assessment, the preliminary efforts on structural mitigation consist of warning equipments and coastal forest planting is conducted. In line with these efforts, close assistantship on strengthening the tsunami awareness and preparedness from district level down to individual/household level is planned. We expect that method and lessons we present in this paper can be applied in other tsunami prone cities in order to reduce the potential loss of life due to tsunami.

## REFERENCES

- ADPC (2007): EVACUATION ROUTES TOOLS ArcGIS toolbox - User's manual.- Italian Ministry for the Environment Land and Sea. Department for Environmental Research and Development, Bangkok, 88 pp.
- Ando, M. (2011): Interviews With Survivors of Tohoku Earthquake, EOS transaction-AGU, 92 (46), 411-412. doi:10.1029/2011GL049580.
- Dengler, L. (2005). The Role of Education in the National Tsunami Hazard Mitigation Program. Natural Hazards, 35(1), 141-153. doi:10.1007/s11069-004-2409-x
- ESRI (2001): ArcGIS (TM) Spatial Analyst: Advanced GIS Spatial Analysis Using Raster and Vector Data., ESRI White Paper, Redlands, 17.
- GIZ-IS (2010a): Planning for Tsunami Evacuations: A Guidebook for Local Authorities and other Stakeholder in Indonesian Communities. <http://www.gitews.org/tsunami-kit/en/E4/tool/Guidebook%20Planning%20for%20Tsunami%20Evacuations.pdf> (July 19, 2012)
- GIZ-IS (2010b): Knowledge and Awareness for Tsunami Preparedness – Introduction. <http://www.gitews.org/tsunami-kit/en/E5/introduction/Introduction%20to%20Knowledge%20and%20Awareness.pdf> (July 19, 2012)
- GIZ-IS (2010c):Guidebook – Dissemination of Tsunami Early Warning at the Local Level in Indonesia. <http://www.gitews.org/tsunami-kit/en/E3/tool/Guidebook%20Dissemination%20of%20Early%20Warning%20at%20the%20Local%20Level%20in%20Indonesia.pdf> (July 23, 2012)
- Hayden, M.H., Drobot, S., et al., 2007. Information sources for flash flood warnings in Denver, CO and Austin, TX. Environmental Hazards 7 (3), 211–219

- Imamura, F., & Abe, I. (2009). History and Challenge of Tsunami Warning Systems in Japan. *Journal of Disaster Research (JDR)*, 4(4), 267-271.
- Johnson, C. W. (2006): Using Computer Simulations to Support A Risk-Based Approach For Hospital Evacuation.
- Khomarudin, R.M., et al. (2010): Tsunami Risk and Vulnerability: Remote Sensing and GIS Approaches for Surface Roughness Determination, Settlement Mapping and Population Distribution Modeling. Dissertation, LMU München: Faculty of Geosciences.
- Klüpfel, H. L. (2003): A Cellular Automaton Model for Crowd Movement and Egress Simulation, Ph.D., Universität Duisburg-Essen.
- McAdoo, B. G., Moore, A., & Baumwoll, J. (2008). Indigenous knowledge and the near field population response during the 2007 Solomon Islands tsunami. *Natural Hazards*, 48(1), 73-82. doi:10.1007/s11069-008-9249-z
- McAdoo B, Dengler L, Titov V, Prasetya G (2006) Smong: how an oral history saved thousands on Indonesia's Simeulue Island. *Earthq Spectra* 22(S3):661–669
- Muhari, A., Diposaptono, S., & Imamura, F. (2007). Toward an Integrated Tsunami Disaster Mitigation : Lessons Learned from previous tsunami events in Indonesia, *Journal of Natural Disaster Sciences (JNDS)*, 29 (1), 13-19.
- Shuto, N., & Fujima, K. (2009). A short history of tsunami research and countermeasures in Japan. *Proceedings of the Japan Academy, Series B*, 85(8), 267-275. doi:10.2183/pjab.85.267
- Spahn et al. (2010): Experience from three years of local capacity development for tsunami early warning in Indonesia: challenges, lessons and the way ahead. In: *Natural Hazards and Earth System Sciences* (10), pp. 1411-1429.
- Strunz, G., et al. (2011): Tsunami risk assessment in Indonesia. In: *Natural Hazards and Earth System Sciences* (11), pp. 67-82.
- Wegscheider, S. et al. (2011): Generating tsunami risk knowledge at community level as a base for planning and implementation of risk reduction strategies. In: *Natural Hazards and Earth System Sciences* (11), pp. 249-258.
- SHUTO, N. (1985) "Effects and limit of coastal forests against tsunami attack," *Proceedings of the Coastal Engineering, JSCE*, 32, 465–469 (in Japanese).

- Gurgel, K.-W., Dzvonkovskaya, A., Pohlmann, T., Schlick, T., & Gill, E. (2011). Simulation and detection of tsunami signatures in ocean surface currents measured by HF radar. *Ocean Dynamics*, 61(10), 1495–1507. doi:10.1007/s10236-011-0420-9
- Börner, T., Galletti, M., Marquart, N. P., & Krieger, G. (2010). Concept study of radar sensors for near-field tsunami early warning. *Natural Hazards and Earth System Science*, 10(9), 1957–1964. doi:10.5194/nhess-10-1957-2010
- Shuto, N. (1993). Tsunami intensity and disasters, in *Tsunami in the world*, Edited by Stefano Tinti, Kluwer Academic Publisher, 197-216 pp
- Harada and Imamura. (2005). Effects of coastal forest on tsunami hazard mitigation – a preliminary investigation. *Advances in Natural and Technological Hazards Research*, Vol. 23 (II), 279-292 pp.
- Lipa, B., Barrick, D., Saitoh, S.-I., Ishikawa, Y., Awaji, T., Largier, J., & Garfield, N. (2011). Japan Tsunami Current Flows Observed by HF Radars on Two Continents. *Remote Sensing*, 3(8), 1663–1679. doi:10.3390/rs3081663
- National Police Agency of Japan (NPA), List of identified victims of tsunami Japan in Miyagi, Iwate, and Fukushima Prefecture. 2011 (in Japanese). Available at: <http://www.npa.go.jp/archive/keibi/biki/mimoto/identity.htm> , last accessed 20 May 2011
- Rudloff, A. lauterjung, J. Munch, U. Tinti, S. (2009). Preface The GITEWS Project ( German-Indonesian Tsunami Early Warning System ), *Natural Hazard and Earth System Sciece-NHESS*, 1381–1382.
- Lauterjung, J., Münch, U., & Rudloff, a. (2010). The challenge of installing a tsunami early warning system in the vicinity of the Sunda Arc, Indonesia. *Natural Hazards and Earth System Science*, 10(4), 641–646. doi:10.5194/nhess-10-641-2010
- Pariatmono. (2012). The Influence of Mentawai Tsunami to Public Policy on Tsunami Warning in Indonesia, *Journal of Disaster Research* Vol. 7 (1), 102-106 pp
- Muhari, A., Imamura, F., Natawidjaja D. H., Post, J., Latief, H., Ismail F. A.: Tsunami mitigation efforts with pTA in West Sumatra Province, Indonesia, *Journal of Earthquake and Tsunami* 4, 341–368, 2010
- Khafid and Handayani. S.: Report of the tide observation during the 2011 Japan tsunami using BAKOSURTANAL stations in Papua, North Molucca and North Sulawesi, National Agency for Survey and Mapping, Internal report, 2011.

- Koshimura, S., Imamura, F., & Shuto, N. (2001). Characteristics of Tsunamis Propagating over Oceanic Ridges : Numerical Simulation of the 1996 Irian Jaya Earthquake Tsunami, 213–229.
- Indonesian Rapid Assessment Team (I-RAPID). (2012). Evaluation of the Indonesian tsunami early warning system on the April 2012 Aceh earthquake. (In Indonesia).
- Japan Rapid Assessment Team (J-RAPID). (2012). Questionnaire Survey after the April 2012 Aceh earthquake.
- Katada, T. (2011). No miracle that 99.8% of the school kids survived: How the children in Kamaishi got through the tsunami. Wedge Infinity <http://wedge.ismedia.jp/articles/-/1334?page=1> last accessed July 30, 2012
- K.R. Newcomb and Mccann, W. R. (1987). Seismic history and seismotectonic of the Sunda Arc, *Journal Geophysical Research*, Vol 92 (4), 421–439.
- Gusman, a. R., Tanioka, Y., Matsumoto, H., & Iwasaki, S.-I. (2009). Analysis of the Tsunami Generated by the Great 1977 Sumba Earthquake that Occurred in Indonesia. *Bulletin of the Seismological Society of America*, 99(4), 2169–2179. doi:10.1785/0120080324
- Polet, J., & Kanamori, H. (2000). Shallow subduction zone earthquakes and their tsunamigenic potential. *Geophysical Journal International*, 142(3), 684–702. doi:10.1046/j.1365-246x.2000.00205.x
- Abercrombie, R. E., Antolik, M., & Felzer, K. (2001). The 1994 Java tsunami earthquake : Slip over a subducting seamount, *Journal of Geophysical Research*, Vol 106 (B4), 6595–6607.
- Tsuji, Y., & Synolakis, C. E. (1995). Field Survey , of the East Java Earthquake and Tsunami of June 3 1994, *Pure and Applied Geophysics*, Vol 144 (3/4), 839-854 pp
- Fritz, H. M., Kongko, W., Moore, A., McAdoo, B., Goff, J., Harbitz, C., Uslu, B., et al. (2007). Extreme runup from the 17 July 2006 Java tsunami. *Geophysical Research Letters*, 34(12), 1–5. doi:10.1029/2007GL029404
- Ammon, C. J., Kanamori, H., Lay, T., & Velasco, A. a. (2006). The 17 July 2006 Java tsunami earthquake. *Geophysical Research Letters*, 33(24), 1–5. doi:10.1029/2006GL028005
- Coppola, D. P. 2007, *Introduction to international disaster management*, Elsevier Publication, 175 pp

- Shuto, N., & Fujima, K. (2009). A short history of tsunami research and countermeasures in Japan. *Proceedings of the Japan Academy, Series B*, 85(8), 267–275. doi:10.2183/pjab.85.267
- Imamura, F.: Tsunami counter-measure in Japan: could people evacuate after receiving a warning?, in “Know Risk,” United Nation – ISDR, 223 pp, 2005
- Bernard, E. N. (2001) The U.S. National Tsunami Hazard Mitigation Program Summary, ITS proceeding, NTHMP review session, pp 21–27.
- Bernard, E. N. (2005). The U. S. National Tsunami Hazard Mitigation Program : A Successful State – Federal Partnership, *Natural Hazard* (35), 5–24.
- Jonientz-Trisler, C., Simmons, R. S., Yanagi, B. S., Crawford, G. L., Darienzo, M., Eisner, R. K., Petty, E., et al. (2005). Planning for Tsunami-Resilient Communities. *Natural Hazards*, 35(1), 121–139. doi:10.1007/s11069-004-2408-y
- Münch, U., Rudloff, a., & Lauterjung, J. (2011). Postface “The GITEWS Project – results, summary and outlook.” *Natural Hazards and Earth System Science*, 11(3), 765–769. doi:10.5194/nhess-11-765-2011
- KOGAMI (2008), Tsunami Alert Community, <http://kogami.or.id/> .
- Rafliana, I. (2012). Disaster Education in Indonesia : Learning How It Works from Six Years of Experience After Indian Ocean Tsunami in 2004, 7(1), 83–91.
- Latief, H., Puspito, N. T., and Imamura, F.: Tsunami Catalog and Zones in Indonesia, *Journal of Natural Disaster Science*, 22(1), 25–43, 2000.Okada 1985
- Imamura, F.: Review of tsunami simulation with a finite difference method, in “Long wave runup models,” H. Yeh, P. Liu, and C. Synolakis, eds., World Scientific, Singapore, 25–42, 1996Roemer et al, 2012
- Aburaya, T. and Imamura, F.: Proposal of a tsunami run-up simulation using combined equivalent roughness, *Annual Journal of Coastal Engineering, JSCE* 49, 276-280. (in Japanese)Muhari et al. (2011).
- Federal Emergency Management Agency (FEMA): Coastal construction manual, Third Edition (FEMA 55), 296 pp., 2003
- Kotani, M., Imamura, F. & Shuto, N.: Tsunami run-up simulation and damage estimation by using geographical information system, *Proc. Coastal Engineering, JSCE* 45, 356–360 (in Japanese)

**THE TOHOKU TSUNAMI OF 11 MARCH 2011 AS RECORDED  
ON THE RUSSIAN FAR EAST****G. V. Shevchenko***Institute of Marine Geology and Geophysics FEB RAS, Yuzhno-Sakhalinsk, Russia***T. N. Ivelskaya***Sakhalin Tsunami Warning Center, Yuzhno-Sakhalinsk, Russia**(Presented at 5<sup>th</sup> Tsunami Symposium of Tsunami Society International (ISPRA-2012) 3-5 Sept. 2012, at EU-Joint Research Centre, Ispra, Italy)***ABSTRACT**

The source region of the catastrophic Tohoku tsunami of 11 March 2011 was near the Russian Far East, thus a warning was issued for threatened coasts of the Kuril Islands and Kamchatka. The tsunami was clearly recorded by a number of coastal tide gauges and by bottom pressure stations (including the Russian DART 21401). The recordings by these instruments were used to estimate the major characteristics of the tsunami waves, including arrival times, maximum heights, duration of signals and main wavelength periods. Further analysis indicated significant differences in the spectral characteristics of the waves propagating eastward toward North America from those directed in a northwest direction, towards the Russian Far East. The main peaks of the eastward propagating tsunami waves were of relatively high frequency, while those propagating in a northwest direction, were mainly of low frequency. At far-field stations, the resonant periods associated with local topographic effects were predominant in the spectra.

**Keywords:** *tsunami, open-ocean DART station, coastal station, arrival time, maximum height, spectra, wavelet analysis*

## 1. INTRODUCTION

The source of the catastrophic Tohoku tsunami of 11 March 2011 was close to the Russian Far East. The tsunami presented a serious threat for the Kuril Islands and Kamchatka so a warning was declared for these regions to evacuate people from low-lying areas and for ships to sail to the open ocean. The tsunami was clearly recorded by a number of coastal tide gauges and bottom pressure stations. A network of precise coastal telemetric gauges, deployed by Russia during the last two years, effectively measured the tsunami at 17 sites – specifically at the Kuril Islands (3), Kamchatka (2), Commander Islands (1), Sakhalin Island (7) and Primorie (4). The tsunami was also recorded by the Russian open-ocean DART station 21401, located east of the South Kuril Islands and by several temporary autonomous bottom pressure stations. The data from DART buoy 21418 located near Japan and buoy 21419 located near the Middle Kuril Islands was used for comparison. These instruments enabled us to estimate major characteristics of the observed tsunami waves, including arrival times, maximum wave heights, duration of the signals and main periods. FFT and wavelet analysis were used to describe the spectral content of the tsunami signals. The present study provides a comprehensive analysis of the middle-field (South Kuril Islands and adjacent northeastern part of Hokkaido Island) and far-field (Kamchatka, Bering and Sakhalin Islands, Primorie) tsunami characteristics on the Russian Far East. The latter area has not experienced a major Pacific tsunami in nearly 50 years. The main goal of the study was to examine the effects of local bottom topography and of coastline geomorphology on the spatial variability of tsunami heights in this particular region of the Russian Far East.

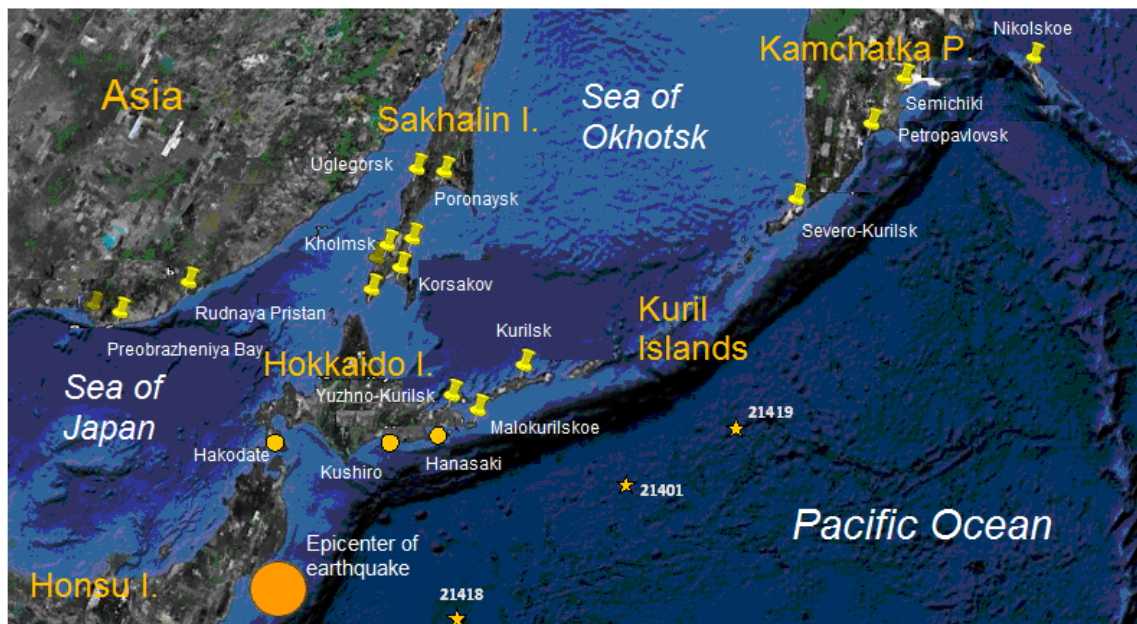


Fig. 1. Stations which recorded the Tohoku 11.03.2011 tsunami. DART stations marked by stars; coastal gauges of the Japanese Tsunami Warning Service marked by yellow circles and Russian TWS coastal telemetric gauges marked by yellow buttons. The earthquake epicenter of earthquake is marked by the orange circle.

## **2. THE TOHOKU EARTHQUAKE AND TSUNAMI**

The great earthquake occurred on March 11, 2011 at 5:46:23 UTC. The US Geological Survey's National Earthquake Information Center (NEIC/USGS) estimate of moment magnitude was  $M_w = 9.0$  with epicenter at  $38.32^\circ$  N,  $142.37^\circ$  E, about 129 km east of Sendai and a focal depth of about 24 km. Tsunami waves ranging up to 12-15 m (up to 30 m in some places) struck the northwest coast of Honshu Island, destroying numerous coastal towns and villages, killing about 20,000 people (precise number of deaths is not determined yet). All recording stations along the stricken area were destroyed and the tsunami wave heights were estimated by the extent of the flooding zone - thus representing approximate values, which may be revised by further surveys.

The most recent catastrophic tsunami in this area of Honshu had been generated by the great earthquake ( $M = 8.4$ ) of March 3, 1933. That particular tsunami was responsible for about 3000 deaths, the destruction of about 6000 buildings and the sinking or destruction of about 12,000 boats (Soloviev and Go, 1974). Most damaged were coastal settlements in the Iwate Province, where tsunami heights averaged from 12~14 m with up to a 29 m maximum. The heights on the coast of Miyagi Prefecture were slightly lower and ranged from 8-12 m with a maximum height of 21 m. At some places of other prefectures, catastrophic tsunami wave were also observed, with heights reported at 19.5 m in Hirota, 26.7 m in Nezaki, etc.

The waves of approximately the same heights were observed on the northeastern coast of Honsu Island in 1611 and 1898, as well. Although the region is densely populated, the high tsunami hazard was largely underestimated – thus the 2011 tsunami caused unprecedented deaths and destructions, in spite of a perfectly functioning Japanese TWS and a good program of public preparedness.

## **3. TSUNAMI CHARACTERISTICS BASED ON THE DATA FROM THE DEEP-WATER DART STATIONS**

In the late 1960s - early 1970s, the Institute of Marine Geology and Geophysics of the USSR's Academy of Sciences (present day IMGG) was the leading organization in the development of near-bottom, hydrostatic pressure recorders. Such recorders were intended for measurements of sea level oscillations on the shelf and in the open sea. The principal aim of experiments in the South Kurils was to determine the characteristics of tsunami waves at different distances away from the shore. Changes recorded in the open sea, where refraction, scattering and other local coastal effects are less intensive, are important in identifying wave field formation peculiarities, caused by processes in the source region of an underwater earthquake. Such measurements help assess tsunami wave enhancement as it approaches the shore and in solving other important problems.

The main initiator of such studies was Academician Sergey Soloviev and the first measuring instruments and experimental applications were made by Victor Zhak (Zhak and Soloviev, 1971). The sea level gauges were deployed in the open ocean and connected by cable with the land-based recorder. Later, autonomous instruments with magnetic storing capability were constructed and similarly deployed. These efforts were implemented in 1980 on the shelf of Shikotan Island and led to the first successful recording of a tsunami in the open ocean (Dykhan et al., 1981). Based on such precise instrumental data, differences between the real tsunami characteristics in coastal and deep-

water environments were identified for the first time. These results - based on deep-water measurements - became the fundamental concept on which the early tsunami warning system functioned. The same operational concept was actively developed and adopted by the Pacific Tsunami Warning Center, headquartered in Honolulu, Hawaii. Presently, the information about deep ocean level oscillations is communicated from the DART stations network, which now covers nearly the entire Pacific Basin and is connected with the national Tsunami Warning Systems using satellite telemetry.

Let us consider the 2011 Tohoku tsunami records from the deep-water stations located in the northwest Pacific, near Honshu and Kuril islands (Fig. 1). DART stations 21401 and 21419 provided quality data. DART station 21418 operated with several singular failures that were corrected in the manual mode. Data provided by DART station 21416 were of low quality and therefore were not used in the present study. The 20-h long (from 4:00 to 24:00) segments were considered and the preliminary calculated tide level was subtracted from the measured values. A similar oscillation pattern was recorded at all stations. First, there was a strong singular wave, and then it was followed by a long sea level oscillation of significantly lower intensity, which was no more than 10 cm in amplitude (Fig. 2).

In all cases, high-frequency oscillations were recorded prior to the main wave arrival (this is typical for recorders of near-bottom hydrostatic pressure, which is changed by seafloor vibrations caused by the seismic Rayleigh wave. DART station 21418 which was the closest to the earthquake epicenter recorded the tsunami arrival at 6:11 UTC, with the main peak at 6:19 (the positive deviation from null average level was 187 cm). In contrast to wind wave theory - which considers the length between trough and crest of a wave - the tsunami study implies that the more important parameter to be estimated is the positive deviation value of the sea level oscillation, which determines the character of tsunami impact on shores and coastal localities as well as the extent of subsequent inland inundation. The negative phase is also important (maximal one was 94 cm at 6:26), since it is related to dynamic loads when the wave backwashes - but this parameter is usually considered separately.

At DART station 21401, which is located beyond the deep-water trench in the area of Iturup Island, the first tsunami arrival was significantly later, at 6:43. The recorded peak wave height here (+67 cm) was recorded at 6:53 and the highest negative deviation (-26 cm) at 7:04. The latest time was when the wave reached the most distant DART station 21419, which is located in the area of Middle Kuril Islands. The peak deviation at this station was +54 cm. at 7:16 and the negative one was -26 cm. at 7:26. This indicates a gentle decrease in wave amplitude as coming from the source - which is usually related to wave front dispersion and attenuation with distance.

To investigate the main periods of tsunami-induced oscillations, the method of spectral-time analysis was used by the present study - a kind of the wavelet analysis STA (Dzienovski et al., 1969), implied for study of changes in spectral amplitudes in time. The calculation was performed for periods from 2 to 100 minutes (frequencies from 0.5 to 0.01 cycles per minute). The matrix of spectral amplitudes was normalized to 30 cm for DART station 21418 and to 10 cm for the two others. The calculation results are illustrated in Fig. 3.

A certain difference in spectral characteristics was derived for different stations which needs to be emphasized. For example at DART station 21418, the signal was generally of high frequency, where the main peak had periods of 6~8 min and the subsequent one had periods of 15~20 min.

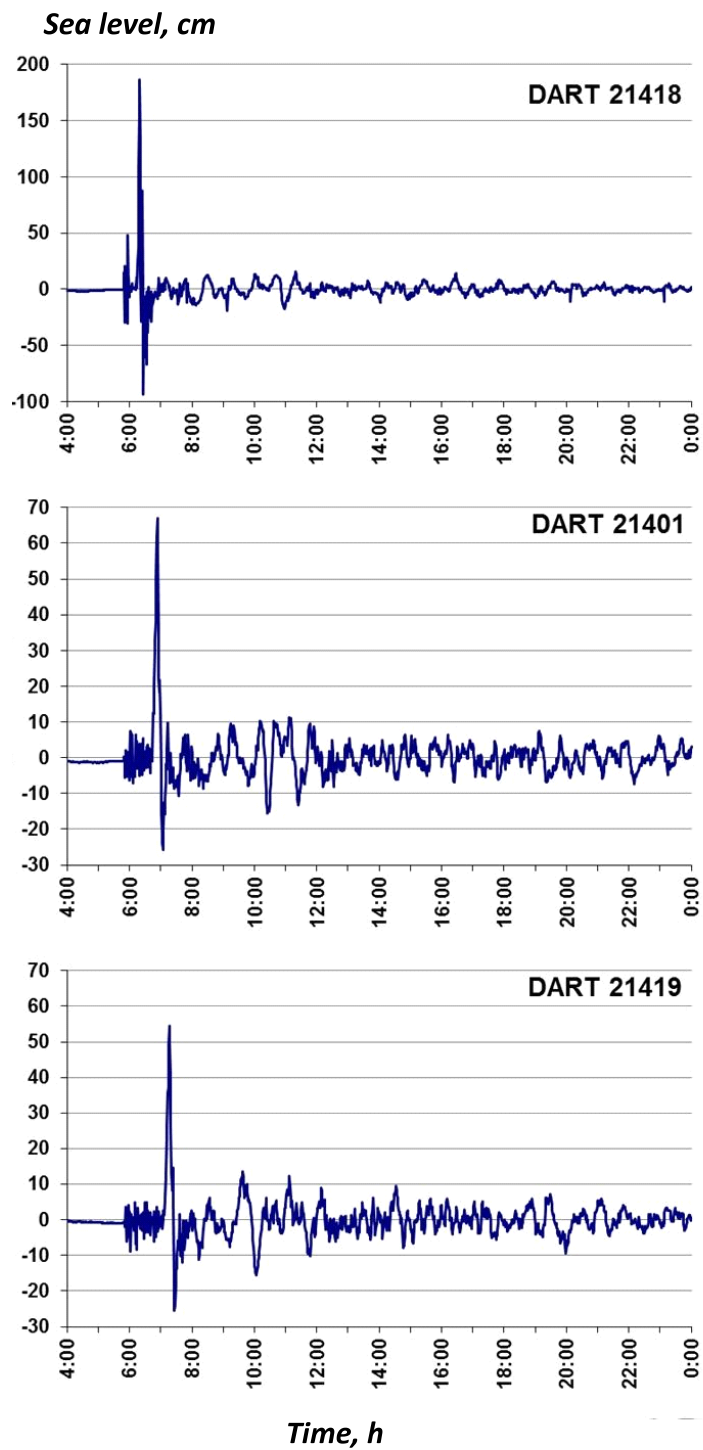


Fig. 2. 20-hour segments of the Tohoku tsunami of March 11, 2011 records, measured by the DART deep-water stations in the Northwest Pacific.

Also noted should be the expressed wave dispersion – specifically the high-frequency vibrations delay in comparison to the longer period components. Such effects are hardly identifiable at near-coastal stations because of the strong influence of reflected and refracted waves in the variable depth zone and the interaction with the coastal boundary. In the open ocean these fine effects are manifested very well in some cases.

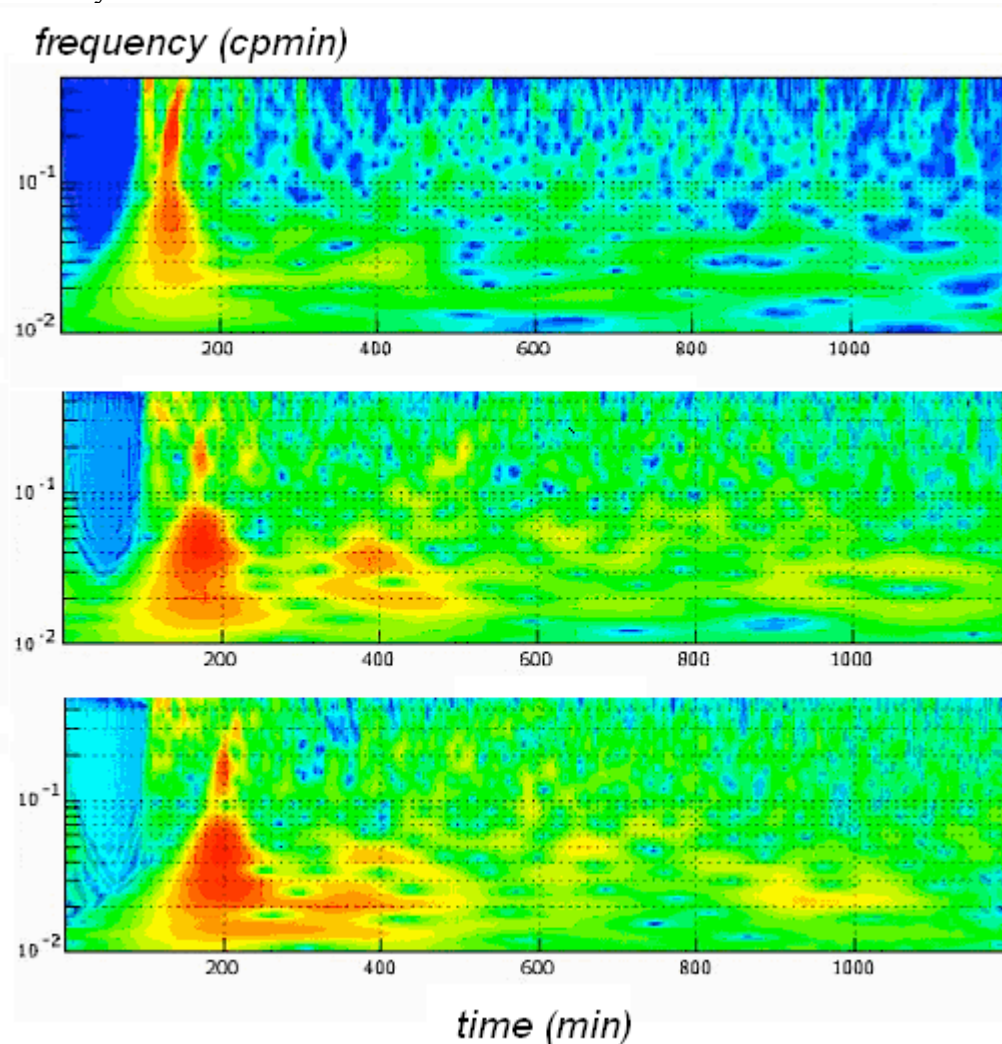


Fig. 3. Spectral-time diagrams of sea level oscillations at DART deep-water stations 21418, 21401 and 21419. The spectra are normalized to the amplitude value of 30 cm for station 21418 and to 10 cm for stations 21401 and 21419. Isolines are drawn with 1 dB step.

The calculated STA-plots were based on observations at DART stations, 214001 and 21419 which are nearly identical and generally have more predominant low-frequency vibrations in comparison to DART station 21418. For example, the main peak was associated with periods of 20~30 min and considerable energy was recorded in the low-frequency part of the spectrum (where the periods ranged from 50~80 min).

Such substantial difference in the energy distribution pattern is typical for a tsunami and is caused by the spatial extent of the source. Longer waves propagate in the direction of the long axis of the source region, while shorter waves, propagate along the shorter axis. The examples presented in this study validate clearly this relationship.

#### 4. MEASUREMENTS OF TSUNAMI BY SHORE-BASED RECORDERS

Tsunamis that propagated towards the South Kuril Islands were first recorded at the Kushiro and Hanasaki stations along Northeast Hokkaido Island, first (Fig. 4a). Measurements of data presented in the Internet with sampling rate of 5 min, did not permit the determination of tsunami arrival time with the desired degree of precision.

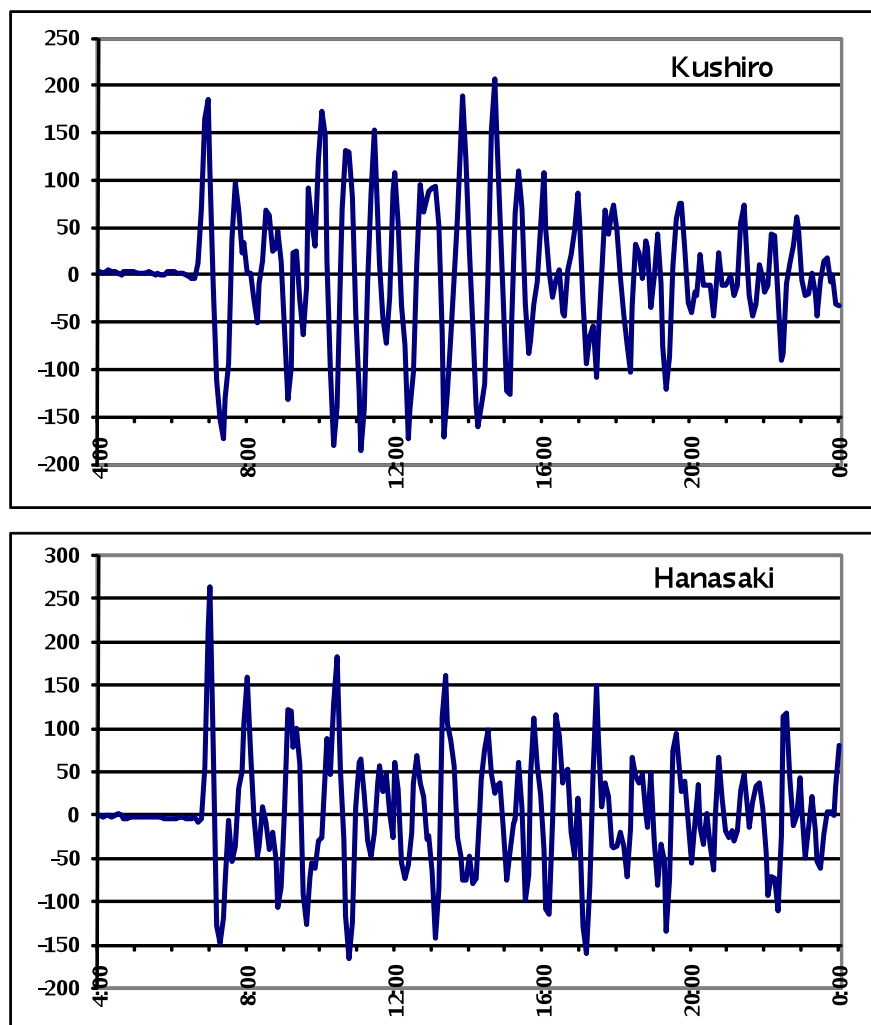


Fig. 4a. 20-hour segments of the Tohoku tsunami of March 11, 2011 records, measured by the coastal stations Kushiro and Hanasaki (northeastern Hokkaido Island).

The first tsunami wave front arrived at the Kushiro station at about 6:25 UTC. The first significant positive deviation from null average level (+185 cm) was recorded at 6:55 and the negative one (-173 cm) 25 min later. Intensive oscillations lasted for a quite long time and the maximum wave height (+207 cm) was recorded at 14:40. Afterwards, the intensity of oscillations decreased significantly, though waves of 50~70 cm in amplitude still were observed for a day.

At the Hanasaki station, the pattern of tsunami manifestation was different. Here, the first wave was clearly distinguished but then the amplitude of the oscillations gently decreased. The arrival time of the first wave front was approximately 5 min later than that at the Kushiro station, the same time interval that was between the first peaks, mainly in Hanasaki (+264 cm). The decreased level of the first wave was also significant (-147 cm at 7:15) and the wave height from trough to crest exceeded 4 m. The amplitudes of subsequent waves were substantially lower, though intensive variations at the Hanasaki station lasted generally for a period longer than those at the Kushiro station, approximately up to 19:30. The last wave of less than 1 m in amplitude was recorded near the end of the day, at 23:30, while on March 12, relatively weak waves of less than 40~50 cm in amplitude were still observed.

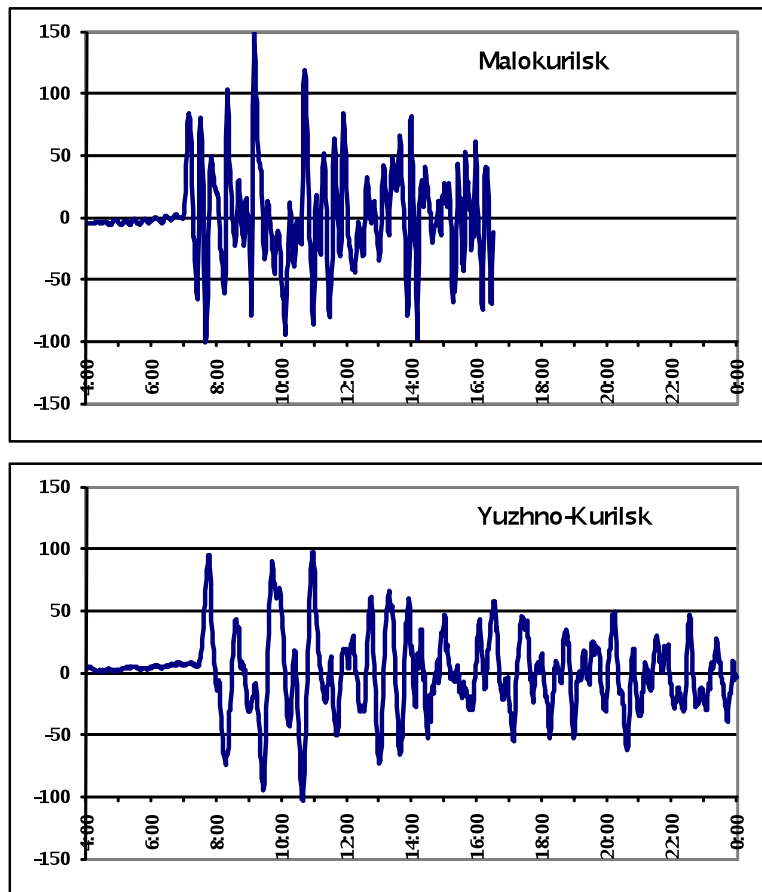


Fig. 4b. 20-hour segments of the Tohoku tsunami of March 11, 2011 records, recorded by the coastal stations of Malokurilsk (Shikotan Island) and of Yuzhno-Kurilsk (Kunashir Island).

Presently, there are three shore-based telemetric TWS sensors on the South Kurils, in Malokurilsk, Yuzhno-Kurilsk, and Kurilsk. The station in Malokurilsk did not operate at the time due to technical problems. The record of shore-based, self-recording, sea level gauge stopped at 16:30 UTC when it run out of ink. However, the most representative part of tsunami-induced oscillations had been recorded. The tide gauge pen-and-paper records were digitized with a 1 min time step and the resulting data used for a statistical and spectral analysis. Fig. 4b represents the plots of 20-h portions of residual (with tide filtered out) of sea level oscillations of the above-mentioned stations.

The record show that the tsunami arrived at Malokurilskaya Bay at 6:50 UTC only 7 min after its arrival time at DART station 21401. This indicates that if a tsunami were generated on the continental slope near the Pacific coast of Japan, then the deep-water sensor would not give any significant time advantage for the initiation of a tsunami warning. The more significant time advantage would be in case of earthquakes in the areas of Kuril Islands, Kamchatka Peninsula or for an event generated at a more distant high-seismic zone of the Pacific. Under the conditions of the March 11, 2011 tsunami, DART station 21401 played the most important role in the TWS operation, since the telemetric sensor in Malokurilskaya Bay was not operating.

The first tsunami wave in this open sea region was quite significant. The positive deviation was +84 cm (at 7:09) and the negative one -67 cm (at 7:24). The highest wave was recorded two hours later at 9:09 (150 cm) and the most significant decrease in sea level (-79 cm) was detected several minutes earlier at 9:04. Thus, the amplitude range between the wave crest and trough was 229 cm. It is interesting to note that the pattern of the March 11, 2011 tsunami manifestation in Malokurilskaya Bay substantially differed from that typical of the open sea area - the latter indicating a predominance of resonant oscillations with periods of about 19 min and an expressly grouped structure. The record in Kurilsk (Fig. 6) is closer to the described type. Observed in this case, are slightly irregular bursts in intensity of variations throughout the entire analyzed portion of the record, though the period of the fundamental mode was the main one. Also identified were non-typical, low frequency oscillations in sea level of about two hours in period.

At Yuzhno-Kurilsk, in-spite of the relatively distant location of the water area discussed above, the pattern of the tsunami wave process was visibly different, due to the predominance of low-frequency oscillations. The wave front reached this station at 7:26, the first significant peak (95 cm) was recorded at 7:45 and the subsequent minimum (-74 cm) was at 8:17. The highest amplitude of the oscillations was observed much later, when the lowest trough (-103 cm) occurred at 10:39 and the peak crest (+98 cm) at 10:57, respectively. In general, the drop in energy was slow and oscillations of about 50 cm in amplitude lasted until the end of the day.

Fig. 5 represents the spectral-time diagrams of oscillations, calculated on the basis of 20-h portions of records at the Hanasaki and Yuzhno-Kurilsk stations. Since the sampling interval of the Hanasaki recorder was 5 min, the minimal possible period of spectral characteristics calculation is 10 min. Therefore, the calculation was carried out for the periods of 10-100 min for all stations. However, this restriction does not appear to be very important, since the high-frequency oscillations did not play a significant role in the tsunami waves observed on the South Kuril Islands.

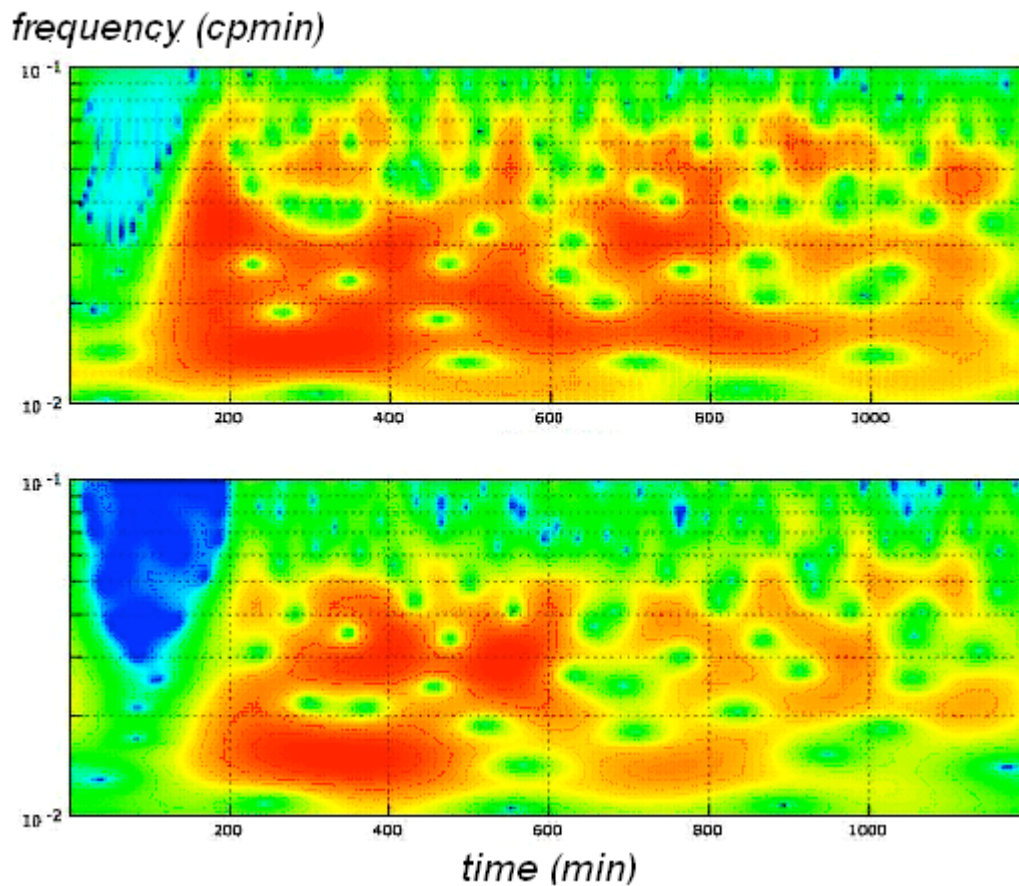


Fig. 5. Spectral-time diagrams for sea level variations at the Hanasaki and Yuzhno-Kurilsk. The spectra are normalized to the amplitude value of 60 cm for the Hanasaki station and to 30 cm for the stations at Yuzhno-Kurilsk. Isolines are drawn with a step of 1 dB.

At the Hanasaki station, the initial segment of the record is characterized by energy increase in a broad range of periods ranging from 20 to 80 min. We can identify the Particular peaks were identified at periods ranging from 25-30 min, 45-50 min and 70-80 min. Low-frequency vibrations had both significant spectral amplitudes (50-60 come) and a long duration, but this peculiarity is notable for the other mentioned peaks, as well.

At the Yuzhno-Kurilsk station, STA-diagram had nearly the same pattern, but with more clearly distinguished two peaks at periods of about 30 and 80 min. Intensification of low-frequency vibrations, manifested at two stations, is typical for the given region and is caused by the absence of shelf resonance. Such intensification is rarely observed, because the excitation of the corresponding component in the initial signal requires a powerful earthquake with large linear size of focal energy propagation. Previously, such case was created when the tsunami of May 24, 1960 caused by the great Chilean earthquake – known at the strongest in the 20th century in the Pacific (Ivel'skaya and Shevchenko, 2006). As has been shown above, the record from DART station 21401 contained the

corresponding component. This indicates that the focus of the March 11, 2011 earthquake near northeast Honshu Island was also of a quite large extent.

The previously mentioned peak in the spectrum at a period of about 30 min might cause significant intensification of the tsunami in Krabovaya Bay (see the effects description below), because the period of its main resonant mode was 29 min (Rabinovich, 1993).

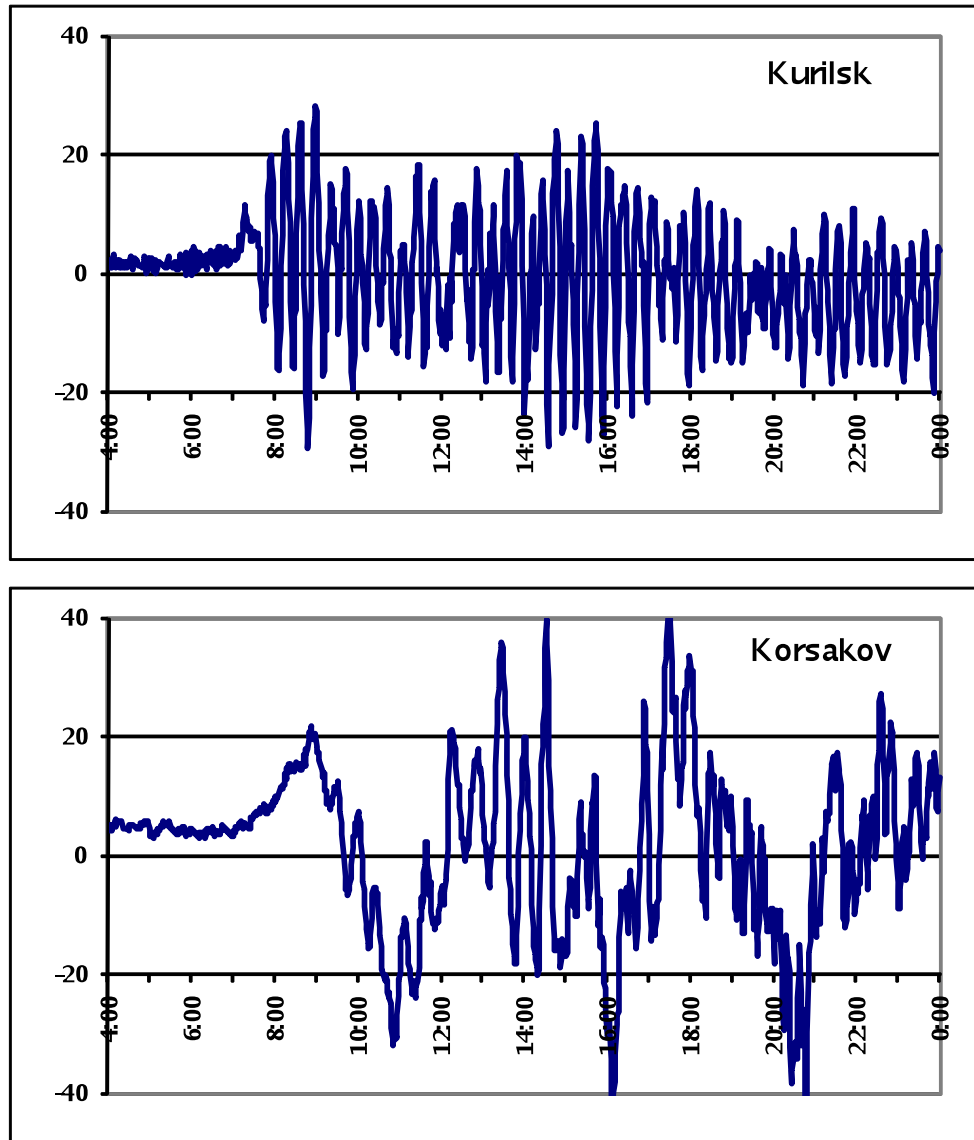


Fig. 6. 20-hour segments of the Tohoku tsunami of March 11, 2011 records, measured by the coastal stations Kurilsk (Iturup Island) and Korsakov (southern Sakhalin Island).

In Kurilsk (Fig. 6), the pattern of the wave process was unordinary for the given area: resonant vibrations of about 20 min in period dominated absolutely and the group wave structure was clearly expressed (wave trains contained 8-10 waves each). Such a pattern of tsunami manifestation is usually observed in bays with narrow entrance, like that at Malokurilskaya (Rabinovich, 1993). However, Kitovyi Bay, where the measuring instruments were placed, is referred to as a semi-closed bay with a long open boundary.

The moment of tsunami wave arrival at this station appeared to be hardly determinable, since it was unclear whether a small positive burst (+11 cm at 7:17) was part of the tsunami. The doubt is caused by the very early appearance of this peak. The highest wave was the fourth in the first wave train (-29 cm at 8:48 and +28 cm at 8:59) and oscillations of nearly the same amplitude were observed in the second wave train in the time period lasting from 14:30 to 16:00.

It is interesting to compare the above-discussed data from shore-based recorders with those from the deep-water station located in the open ocean near Iturup Island. Only the pattern at the Hanasaki station demonstrates certain resemblance with signal, non-distorted by shelf-related and coastal effects (this mainly related to the shape of the first wave). At all the other stations, the influence of local relief is so significant that it is impossible to identify any resemblance. This emphasizes the most important role played by the bottom relief peculiarities at the zone of sharp depth changes in the pattern of tsunami propagation; however, this is a factor that is often underestimated.

In Severo-Kurilsk, the telemetric sensor was switched off a day before the tsunami for the preventive maintenance and then switched on again in the morning of March 12. In spite of the interruption, a wave of more than 80 cm in height was detected. In Petropavlovsk-Kamchatsky, due to the narrow strait, tsunami waves in the Avachinskaya Bay are usually substantially lower than in the open parts of the coast. This phenomenon was observed on March 11. The amplitude of sea level oscillations did not exceed 15 cm. In contrast to this, at the Semyachiki station in Kronotsky Bay, the maximum wave height was significant (82 cm at 15:28). At 8:37 the wave reached Nikolskoe port (Bering Island) and at 9:03 its height became maximum (25 cm). Subsequently, oscillations in wave height were quite long but with a small amplitude (15-20 cm).

Clear records of the tsunami were acquired on the south and southeast coasts of Sakhalin Island. In Korsakov port, the tsunami wave arrived at about 7:40 (Fig. 6). Here, very low-frequency sea level oscillations with period about 4.7 hours were observed, which are related to the zero resonant mode of Aniva Bay and are usually predominant when tsunami strikes. This peculiarity manifested on March 11, 2011, as well. The maximal wave in amplitude was detected much later than the tsunami arrival (-42 cm at 16:09 and +47 cm at 17:30). At the Kril'on Cape station, which is located in the vicinity of a nodal line of the bay's main mode, oscillations were substantially more high frequency and relatively weak (the amplitude did not exceed 15 cm).

In the record from the Starodubskoe station, a clear moment of wave arrival cannot be identified - however, it was most likely at 8:05. The first well-expressed peak occurred at 8:44 (24 cm). The maximum wave height (+33 cm) was observed much later, at 15:10, while the maximum amplitude between the crest (+30 cm at 22:34) and trough (-31 cm at 21:51) was detected more than 7 hours later.

In Poronaysk, the tsunami-caused oscillations were of similar pattern, but manifested much later. The arrival time of the wave front was detected at 10:06 and the first well-expressed peak (+38 cm) was observed at 10:38, nearly 2 hours later than at the Starodubskoe station. Such a big time shift

between the relatively close points is caused by significant propagation time of long waves within the shallow-water Terpeniya Bay, in whose farthest corner the Poronaisk station is located.

The maximum amplitude of oscillations was identified here more than 7 hours after the first wave arrival: at 17:11 for the minimum (-33 cm) and at 17:53 for the maximum (+44 cm). Intensive oscillations at this point lasted for about a day. For example, the wave of nearly same amplitude was detected about a half-day after the first maximum (+35 cm at 8:51 and -37 cm at 9:26 on March 12).

Let us consider the peculiarities of Tohoku tsunami penetration into the Sea of Japan. The Tsugaru Strait that divides Hokkaido and Honshu islands is located close to the source and, despite its narrow width and complex pattern of coastline, possesses a good conducting ability because of its sufficient depth. The first wave arrived at the Hakodate port in this strait approximately an hour after the earthquake, at about 6:45. The maximum of the first wave (+163 cm relative to the average level) was detected at 7:35 and 20 min after this the sharp decrease in level (-131 cm) occurred. The maximum amplitude of oscillations was observed two hours later (+203 cm at 9:55, -155 cm at 10:15). Another high wave (+226 cm) was detected much later, at 16:35.

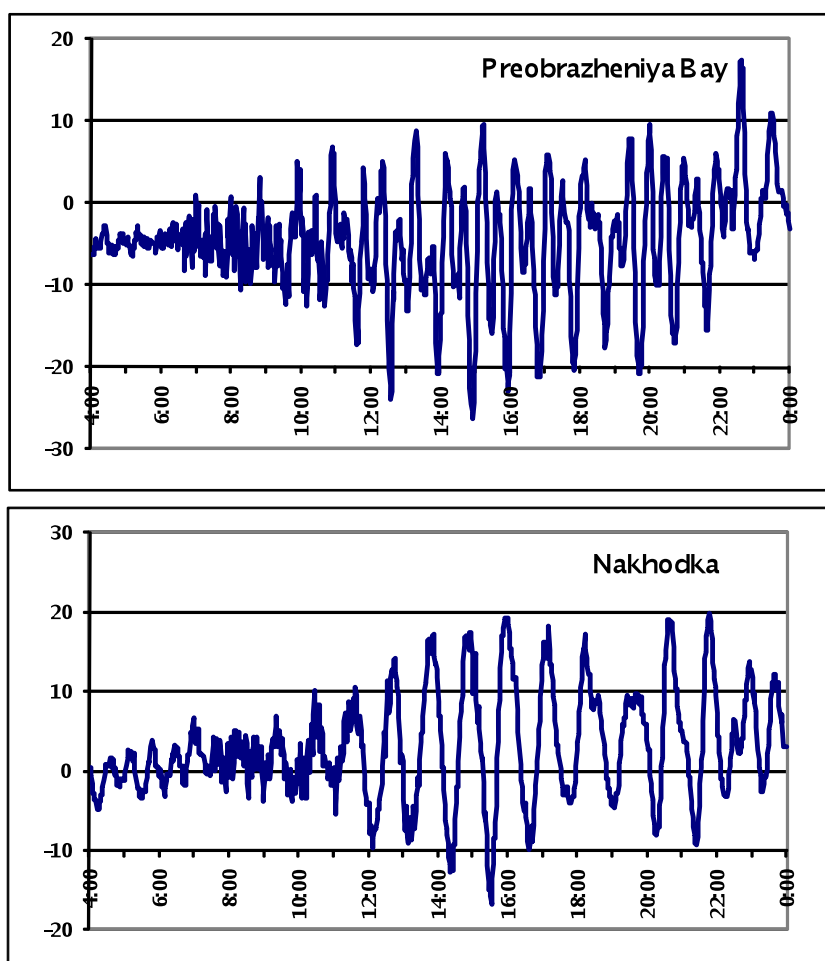


Fig. 7. 20-hour segments of the Tohoku tsunami of March 11, 2011 records, measured by the coastal stations Preobrazheniya Bay and Nskhodka (Primorie).

The tsunami was recorded by shore-based instruments in Primorye (Nakhodka, Preobrazheniya Bay, Rudnaya Pristan) and on west coast of Sakhalin Island (Nevelsk, Kholmsk, Ulegorsk). Determination of tsunami arrival time at these points was very difficult, since the intensity of tsunami-related oscillations was relatively small and the level of long-wave noise had increased (most likely due to weather deterioration) several hours prior to tsunami arrival. It is firmly believed that the first tsunami-related peak was +4 cm at 8:48 (see Fig. 7), which is slightly more than an hour later than the wave arrival at the Hakodate station. In Nakhodka Bay, the tsunami wave arrived at about 9:00 local time and the first maximum (+6 cm) was at 9:20. The maximum oscillations at this location were observed much later: in Preobrazheniya Bay, the minimum (-26 cm) was detected at 14:55 and the maximum (+10 cm), at 15:14. In Nakhodka Bay the minimum (-17 cm) and the maximum (+19 cm) were at 15:32 and 15:59, respectively. Generally, at the similar pattern of intensity oscillations with time for these two stations, a visible difference in predominant periods is notable: about 0.5 h in the Preobrazheniya Bay and about 1 h in the Nakhodka Bay. These differences are caused by resonant properties of these water areas, due to their spatial extent and depth. In Rudnaya Pristan, resonant oscillations of about 1 hour in period also dominated and their maximum amplitude was 15 cm.

Tsunami waves reached the southwest coast of Sakhalin Island much later than the Primorye coast. For example, the southernmost station in Nevelsk detected the first positive deviation (+9 cm) at 10:58 and stable oscillations dominated in the record. This is quite extraordinary phenomenon, since there is no bay in this area (since it is in bays, where stable oscillations of resonant type can manifest). The highest wave amplitude was 27 cm (+15 cm at 14:56 and -12 cm at 15:10).

The most distant station in Ulegorsk recorded tsunami wave arrival at about local midday, but the intensity of waves increased much later. For example, the highest amplitude was the minimum -3 cm at 22:04 and the maximum +15 cm 22:19. In the records, the stable oscillations of about 50 min in period were identified - which may be most likely related to the transversal seiche of the Tatar Strait.

## 5. CONCLUSIONS

The present study analyzed a great volume of instrumental measurements data of the Tohoku tsunami on March 11, 2011, as acquired at the deep-water and shore-based sensors in the Russian Far East. The great difference between the signal in the open ocean and in the coastal zone has been visually illustrated. In the former case, powerful singular pulses and subsequent relatively weak oscillations were observed, while the long-term intensive oscillations were recorded in the latter case (only at the Hanasaki station the first wave was of maximal height). The pattern of variations near the shore was determined mainly by local topography; the general properties caused by the processes of the tsunami source manifested less intensively.

Resulting from the analysis of deep-water stations data, was determined that shorter waves (with main peaks of 6-8 and 15-20 min) propagated eastwards, to the open ocean side, while longer waves (with main peaks of 25-30 min) radiated to the side of Kuril Islands; the significant energy was identified in the low-frequency part of spectrum at periods ranging from 50-80 min. The low-

frequency component significantly intensified on the extended shelf of the South Kuril Islands and played an important role in the formation of tsunami-caused oscillations at the Hanasaki, Malokurilskoe and Yuzhno-Kurilsk stations. In far field, the local topography effect manifested differently: the most important role in tsunami-caused oscillations was due to bays' resonant modes.

In the most investigated points (in densely populated settlements of Yuzhno-Kurilsk, Malokurilsk and Severo-Kurilsk) the tsunami heights ranged from 2-2.5 meters. The highest waves were detected in Krabovaya Bay, Shikotan Island (about 3 m). Most likely, this was caused by the presence of the peak at the period of about 30 min in the initial signal. Such period is close to the period of the bay's main mode and this proximity led to resonant strengthening of the sea level oscillations.

The Tsunami Warning issued from the Sakhalin TWS for the localities on Kuril Islands was reasonable, because such wave heights were of a serious danger for vessels in the ports, as well as for workers at industries and local inhabitants in the coastal zone.

## REFERENCES

- Dykhan, B.D., Zhak, V.M., Kulikov, E.A. et al. (1983), Registration of tsunamis in the open ocean// *Marine Geodesy*, **6**, 303-309.
- Dzienovski A., Bloch S. and Landisman M. (1969). Technique for the analysis of transient seismic signals// *Bull. Seism. Soc. Am.* **59**, 427-444.
- Ivelskaya, T.N., and Shevchenko, G.V. (2006). Amplification of low-frequency component of Chilean tsunami (May 1960) on the northwestern shelf of Pacific Ocean// *Russian Meteorology and Hydrology*, **2**, 69-81. (in Russian, English translation).
- Rabinovich, A.B. (1993). Long ocean gravity waves: trapping, resonance, and leaking, *Gidrometeoizdat*, St. Petersburg, Russia (in Russian).
- Soloviev, S.L. and Go. Ch.N. (1974). Catalogue of Tsunamis on the Western Shore of the Pacific Ocean, *Nauka Publ. House*, Moscow (in Russian; English translation).
- Zhak, V.N., and Soloviev, S.L. (1971), Distant registration of tsunami type weak waves on the shelf of the Kuril Islands// *Dokl USSR Acad. Sci., Earth Science*, **198** (4), 816-817 (in Russian, English translation).



**RESPONSE OF THE GDACS SYSTEM TO THE TOHOKU EARTHQUAKE AND  
TSUNAMI OF 11 MARCH 2011**

**Annunziato, G. Franchello, T. De Groeve**

*EC-Joint Research Centre (EC-JRC), Italy*

*(Presented at 5th Tsunami Symposium of Tsunami Society International (ISPRA-2012) 3-5 Sept. 2012, at EU-Joint Research Centre, Ispra, Italy)*

**ABSTRACT**

The Tohoku Tsunami of 11 March 2011 was successfully identified and classified as Red alert by the GDACS system only when reliable and more correct estimations of the originating event have been provided to the system by the international seismological networks. Nevertheless the early analysis of the event by the comparison of the scenario calculations with the sea level could give important information on the real extent and impact of the Tsunami. The paper describe the response of the GDACS system and identify the lessons learned that determined changes in the logic and the procedures of the Tsunami calculations strategy.

**Keywords:** *Early Warning Systems, Tsunami, Propagation, Inundation, Alerting*

## 1. INTRODUCTION

A large earthquake occurred off shore the Pacific coast of Tohoku, Japan ( $38.1035^{\circ}\text{N}$ ,  $142.861^{\circ}\text{E}$ , M 9.0 at 5:46:18 UTC on March 11, 2011, and generated a large tsunami and caused more than 15000 fatalities and more than 4500 missing, in the east coast of Japan (Fuji et al, 2011). USGS identified the fault mechanism as dipping thrust with strike parallel close to the Japan Trench. The fault movement caused large movements of the earth crust. Continuous measurements of GPS indicated a subsidence of about 1.2 m, close to Central Myagi (Geospatial Information Authority of Japan (GSI)). Several organizations issued Tsunami Alerts for this event; the first was the Japanese Meteorological Agency (JMA) that is in charge in Japan of officially alerting the local communities of potential damaging tsunami events. However the alerting, due to an underestimated initial magnitude of the event, was not indicating the right potential sea level height and was misinterpreted from some of local residents. This paper describes the response of the European Commission's Global Disasters Alerts and Coordination System (GDACS) response to this event.

The Joint Research Centre of the European Commission is operating the Global Disasters Alerts and Coordination System (GDACS, <http://www.gdacs.org>) since 2003. This system, jointly developed by the European Commission and the United Nations, combines existing web-based disaster information management systems with the aim of alerting the international community in case of major sudden-onset disasters and thus facilitating the coordination of international response during the relief phase of each disaster. When new natural disasters events occur, automatic analysis reports are created and sent to users by mail, fax or sms.

As a consequence of the 26 December 2004 tsunami, JRC included the tsunami modeling in the GDACS system in order to improve and complete the automatic reporting system. At the beginning of 2005 a travel time wave propagation model was included (Annunziato 2005). This model calculates the wave arrival times - independently on the initial tsunami wave height. In 2006 a new analytical tool has been developed in order to provide also the wave heights and thus identify the locations with higher risk of tsunami damage (Annunziato, 2007). The model is based on the SWAN propagation code (Mader, 2004), surrounded by a series of systems to automatically react to events and initialize and post-process the code calculations.

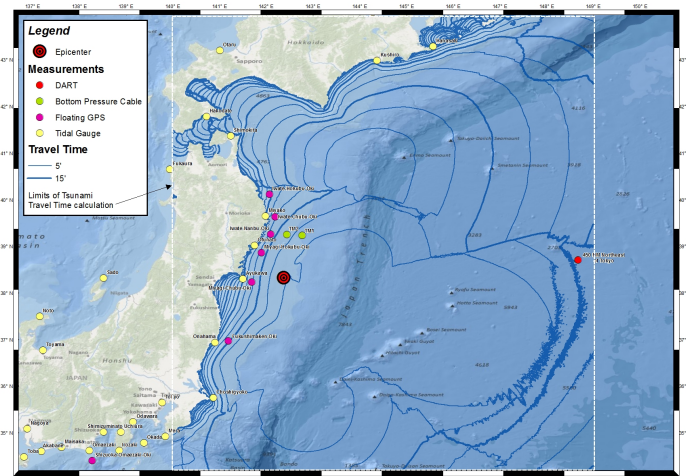


Figure 1 – Identification of the epicenter and several sea level measurements in Japan. The blue curves represent the travel time isochrones each 5 min.

When a potential tsunami occurs (from an earthquake with magnitude greater than 6.5, Richter scale) with epicenter under the water or close to the shoreline (i.e. so that part of the deformation occurs under water), an estimate of the potential consequences of the event is performed and, if the estimated height exceeds certain threshold, an alert is issued and sent to the registered users of the system (20,000 as of July 2012). The initial estimate is based on a pre-calculated scenario composed of 136,000 calculations covering all the potential tsunami sources based on historical catalogs. The epicenters have been obtained creating a grid of 10,168 locations at distance 0.5 min each other, around the historical events and performing 13 calculations, from 6.5 to 9.5 for every 0.25 min. The initial fault in the Mod 1 database is a simple co-sinusoidal function with maximum height equal to the maximum expected deformation for that magnitude and as such it may be considered as a worst-case scenario. A new database is in preparation considering the Okada model for the deformation and historical fault mechanisms.

## **2. THE GDACS SYSTEM**

The Global Disaster Alert and Coordination System (GDACS), is a web-based platform that combines existing web-based disaster information management systems with the aim to alert the international community in case of major sudden-onset disasters and to facilitate the coordination of international response during the relief phase of disaster. GDACS is jointly developed by the JRC and the United Nations Office for Coordination of Humanitarian Affairs (OCHA). (De Groeve et al., 2006, De Groeve, 2007). GDACS comprises of three elements: 1) Web based automatic alert notifications and impact estimations for earthquakes, tsunamis, tropical cyclones, volcanic eruptions and floods. 2) A community of emergency managers and emergency operation centers in responding and disaster-prone countries and disaster response organizations worldwide. 3) Automatic information exchange in web-based disaster information systems. (De Groeve et al., 2009).

The GDACS portal has been built at the Joint Research Centre and available at <http://www.gdacs.org>. It has integrated GDACS compliant information sources and offers a way to register for alert services by email, fax, SMS and/ or RSS as provided by GDACS components. GDACS has 20,000 active users of 184 countries. It has alert and monitoring system for earthquakes and tsunamis, tropical cyclones, volcanic eruptions and floods (De Groeve et al., 2006).

GDACS tsunami alert calculations are triggered by earthquakes that occur in or near water. The logic for the tsunami alert is based on (1) the magnitude and location of the earthquake, (2) the depth of the earthquake, (3) the maximum wave height at any coast reach by the tsunami. The first two parameters are used to look up a tsunami wave height calculation in the JRC Tsunami Database (containing over 132,000 scenarios). For each earthquake of magnitude exceeding 6.5 which occurred in a location under water or close to the shoreline, the tsunami database is queried for the closest matching scenario. Scenarios have been calculated for 10,180 locations covering tsunamigenic regions (from NOAA database) for magnitudes ranging from 6.5M to 9.5M with steps of 0.25M for a total of 136,000 scenarios. If a scenario is available, the maximum wave height at a coast is retrieved. The alert color depends on the maximum wave height according to the following table:

Height (m)		Alert Level
Min	Max	
0	1	Green
1	3	Orange
3		Red

If no scenario has been pre-calculated (only very few cases), the IOC alert matrix is used, based only on earthquake magnitude. This fallback routine, although widely used in tsunami warning centers, results in too many false alerts, therefore the first method is preferred (GDACS, 2010). In any case, after every event - if the scenario exists or not - an automatic online calculation is performed that is useful for a quick analysis but is not useful for the alerting, as the results are available only 20-30 min later.

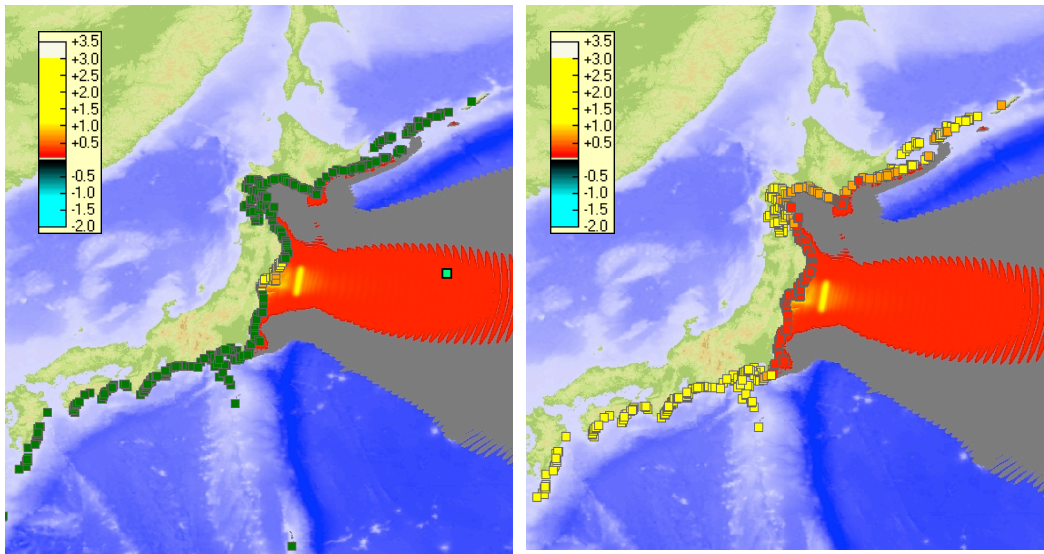
Alert color	Magnitude and depth	Tsunami risk (max height)	Delay	Source
	7.9M, 24.4km	2.1m (at 06:18)	00:20	NEIC
	7.9M, 10.0km	1.8m (at 06:29)	00:20	NEIC
	8.8M, 24.4km	8.6m (at 06:21)	00:42	NEIC
	7.9M,10km	1.8m (at 06:29)	00:43	JMA
	8.8M, 24.4km	8.6m (at 06:21)	00:46	NEIC
	8.8M, 24.4km	8.6m (at 06:21)	00:48	NEIC
	8.8M, 24.4km	8.6m (at 06:21)	00:50	NEIC
	8.4M, 10.0km	5.2m (at 06:22)	02:22	JMA
	8.8M, 24.4km	8.6m (at 06:21)	00:53	NEIC
	8.8M, 10.0km	8.1m (at 06:25)	04:02	JMA
	8.9M, 24.4km	11.9m (at 06:15)	01:08	NEIC
	9.0M, 32.0km	11.6m (at 06:15)	3d	NEIC

Table I – timeline of the events detected by GDACS and the related automatic

### 3. TSUNAMI ESTIMATIONS FOR THE 11/3/2011 EVENT

In the case of the Japan event of 11/3/2011, the first estimate was obtained 20 minutes after the event with one introduced by USGS into the JRC system (Table I), with parameters 142.369 longitude, 38.3215 latitude and magnitude 7.9 Mw, depth 24.4 km. The initial calculation adopted by GDACS was the calculation identified by the code DISK3/MAG\_800/P1425^P0385^0800 which corresponded, in the logic of the GDACS grid storage format to P1425 or +142.5 longitude, P0385 or +38.5 latitude and 0800 or Magnitude 8. This calculation indicates a maximum height of 2.1 m reduced to 1.62 m due to the depth of 24.4 km, in the location Kamaishi, Japan (Fig.1). This value of maximum height called for an Orange alert, automatically sent out to all GDACS users within 20 and 30 min from the event occurrence.

The analysis of the closer DART (Fig. 3) showed that the peak was reached at 6:17 UTC (i.e. 31 min after the event). Considering the delay in the data collection from the buoy which was in the order of 5 min, we knew that the peak was much higher than the values estimated by the online calculation (green curve in Fig. 3) only at 6:23 UTC. In order to get the right value of height, the curve should be multiplied by a value 14. In Ofunato (Fig. 4) the reading went off-scale and could not be possible to compare with the value of the online calculation.



Online calculation results using the initial values of M 7.9 and depth 24.4 km

Online calculation results when multiplied for a factor 14 (only the locations color code is multiplied)

Fig. 2: Maximum estimated height with the online calculation

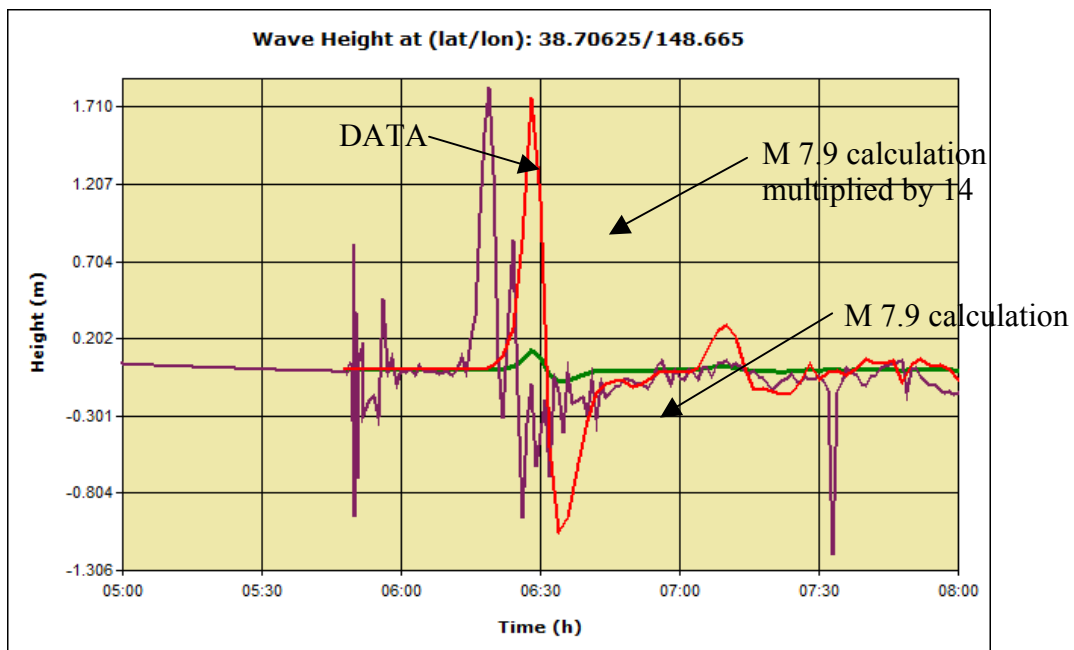


Fig. 3: Sea level estimated on DART 450 NM Northeast of Tokyo (brown curve), compared with the first online calculation (green curve) and the same curve multiplied by a factor 14.

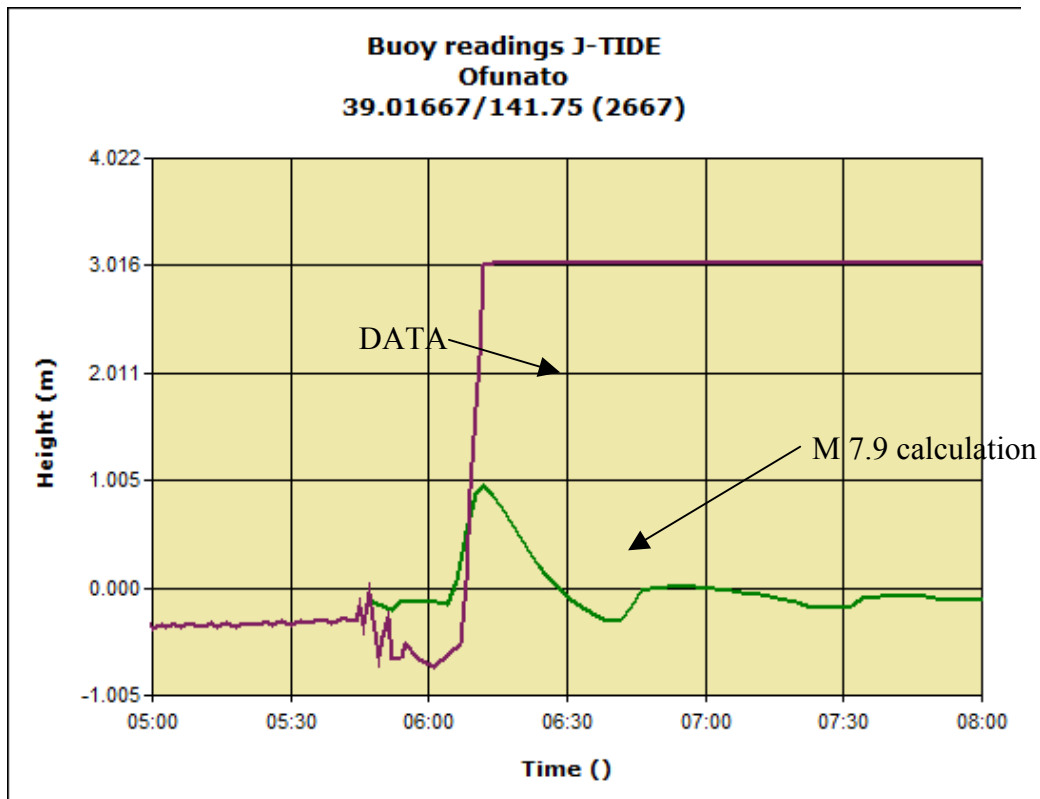


Fig. 4: Sea level estimated on mareograph in Ofunato

The value of 14 in the sea level allowed making the following consideration. Considering that the energy is proportional to the maximum sea level, the above comparison suggests that the energy was 14 times larger than the one corresponding to magnitude 7.9 and the same for the moment magnitude  $M_0$ . The correlation between magnitude and moment magnitude is

$$M_w = \frac{2}{3} \log(M_0) - 10.7$$

If the new Moment Magnitude  $M_0'$  14 times greater than the one for Magnitude 7.9 it means that the new magnitude will be:

$$M_w' = \frac{2}{3} \log(M_0 \times 14) - 10.7 = \frac{2}{3} \log(M_0) - 10.7 + \frac{2}{3} \log(14) = M_w + \frac{2}{3} \log(14) = 7.9 + 0.76 = 8.6$$

This means that the real magnitude had to be at least 8.6 instead of 7.9. Therefore an email to the Monitoring and Information Center (MIC) in Brussels was sent at 6:26 UTC that the estimated magnitude was in the order of 9.0 and that all the possible alerting had to be given.

Few minutes after, at 6:28 UTC we were notified that the magnitude was increased to 8.8. This new estimate of the magnitude called for another re-evaluation of the alert level by GDACS

through the scenario matrix, which now estimated a maximum height of 8.6 m, which meant a Red Alert in the GDACS logic ( $h > 3\text{m}$ ). Therefore a new alert was issued and sent to all the 20,000 GDACS users between 42 and 52 minutes after the event. Much later the event was finally revised to a magnitude 9, after several intermediate revisions; for each revision a new online calculation was performed but no additional alert was sent out because the alert level was not modified and remained Red.

#### 4. POST EVENT CALCULATIONS

Several calculations were performed in the hours after the event in order to identify where the most of the damage occurred.

##### *4.1 Calculations with focal mechanism*

A few hours after the event the focal mechanism for this earthquake has been published by USGS and the most probable solution was: depth 32 km, strike 187, dip 14 and rake 681. The width and length assumed for the dislocation area were estimated at 500 km in length and 140 km in width, a rectangular area obtained by available empirical relations of scaling law (Utsu et al., 2001), from magnitude of the earthquake, which can be expressed as follows:

$$\text{Log } L = 0.5 \text{ Mw} - 1.8$$

$$\text{Log } W = 0.28 L$$

where  $L$ ,  $W$ ,  $M$  and are fault length (km), width (km) and magnitude ( $M_w$ ). The results of the comparison with the sea level data is shown in Fig. 5 and shows that the agreement is better than with the scenario calculation but is not yet perfect. The height is underestimated and the peak is wider than in the real case. Also a double peak is not shown. The same plot shows the comparison with the inversion technique that will be described later.

The comparison with the sea level in South Iwate (Fig. 6) shows more clearly that the simple single fault focal mechanism calculation is unable to correctly describe the double sea level increase. Also is not able to show the initial sea level decrease present in the data.

It should be noted that all the measured data have been corrected in order to take into account the initial deformation (Annunziato, 2012).

---

<sup>1</sup> [http://earthquake.usgs.gov/earthquakes/eqinthenews/2011/usc0001xgp/neic\\_c0001xgp\\_cmt.php](http://earthquake.usgs.gov/earthquakes/eqinthenews/2011/usc0001xgp/neic_c0001xgp_cmt.php)

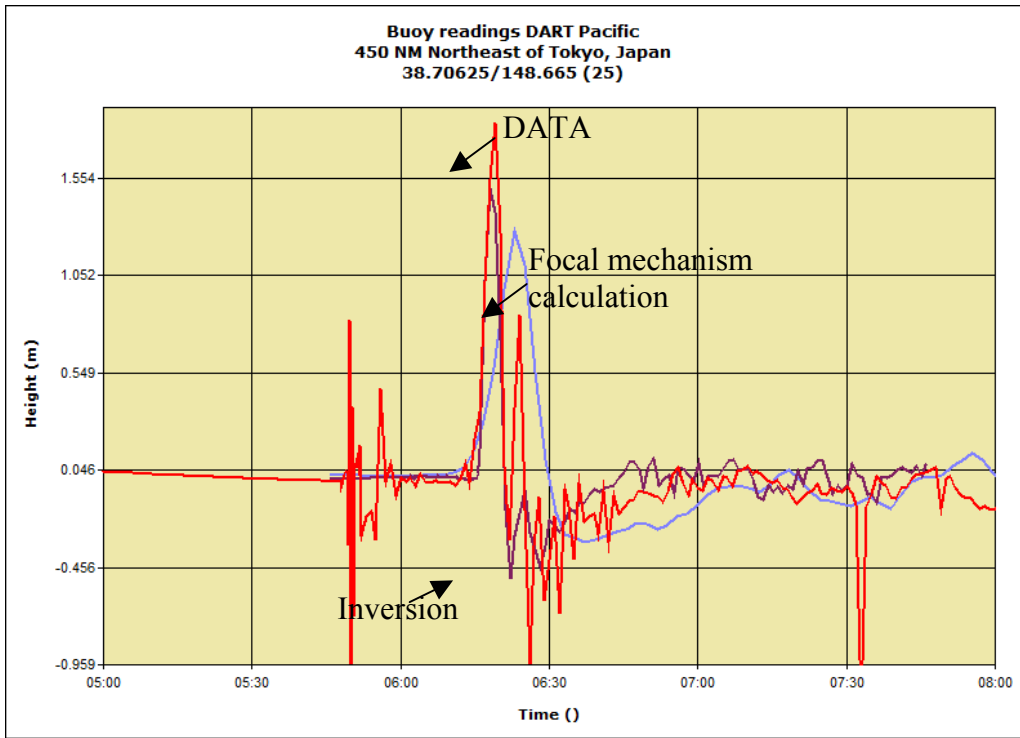


Fig. 5: Sea level estimated on the DART 450 NM NE of Tokyo

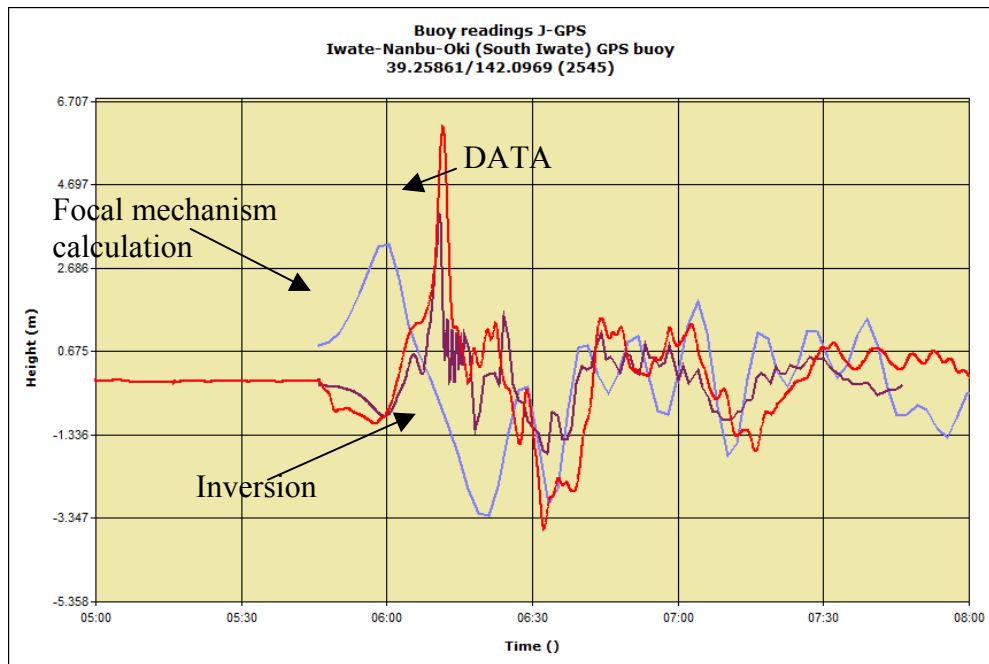


Fig. 6: Sea level estimated on GPS South Iwate

## 4.2 Inundation Analysis

During the same day of the event we started to perform inundation calculations in order to identify which were the areas potentially mostly affected. The calculations have been performed with the SWAN-JRC code coupled with the Hyflux code for the inundation part (Franchello 2008, 2010 and Franchello et al, 2012).

As the tsunami affected the Eastern coast of Honshu, the analysis subdivided it in three regions of different topography and geographical characteristics. The northern region (1) is mountainous. The tsunami did not reach far inland, but waves were amplified in the many coves. The middle region (2) is flat and densely populated. The southern region (3) is relatively far from the tsunami, but was affected by large aftershocks.

The table below shows the population characteristics of the three regions. Coastal population was identified as living below 5m (using SRTM as a data source for elevation) and within 10km of the coast. Flooded population areas were identified by the HyFlux2 tsunami model. In region 1, the flooded population area is larger than the coastal population because the tsunami was higher than 5m.

	Population		
	Total	Coastal below 5 m	Flooded
Region 1	808 140	69 205	108 215
Region 2	2 578 489	533 755	480 633
Region 3	2 336 596	374 496	187 075
<b>Total</b>	<b>10 249 918</b>	<b>1 143 616</b>	<b>542 071</b>

Flooded area and population are calculated in the three frames (table), validated with remote sensing results in the Sendai area. Figures are compared with the total population in the map extent, and with coastal population living below 5m within 10km of the coast.

Table 2 – Impact of Tsunami Inundation, as estimated the day of the event

From this analysis, the total population living in flooded areas was determined to be more than half a million. This is consistent with reports of people in shelters. While most people are from the Sendai area (region 2), the other regions also have 100,000 and 180,000 affected people.

The most populated region is Miyagi, with the city of Sendai with a population of around 230,000. The relatively flat coastal area caused tsunami waves to increase in height near the shore, reaching more than 15 m. The water inundated up to 4 km inland, fig. 7.

The calculations of JRC match results obtained by interpretation of satellite images. We compared with an analysis of the Colorado Flood Observatory and the National Geospatial

Intelligence Agency (NGA), both published on 13 March 2011. More recent results published by UNOSAT (based on RADARSAT imagery) confirm the accuracy of the JRC analysis. It should be noted that these analyses were performed the same day of the event and therefore could not benefit of the large amount of post Tsunami Survey data that have been produced.

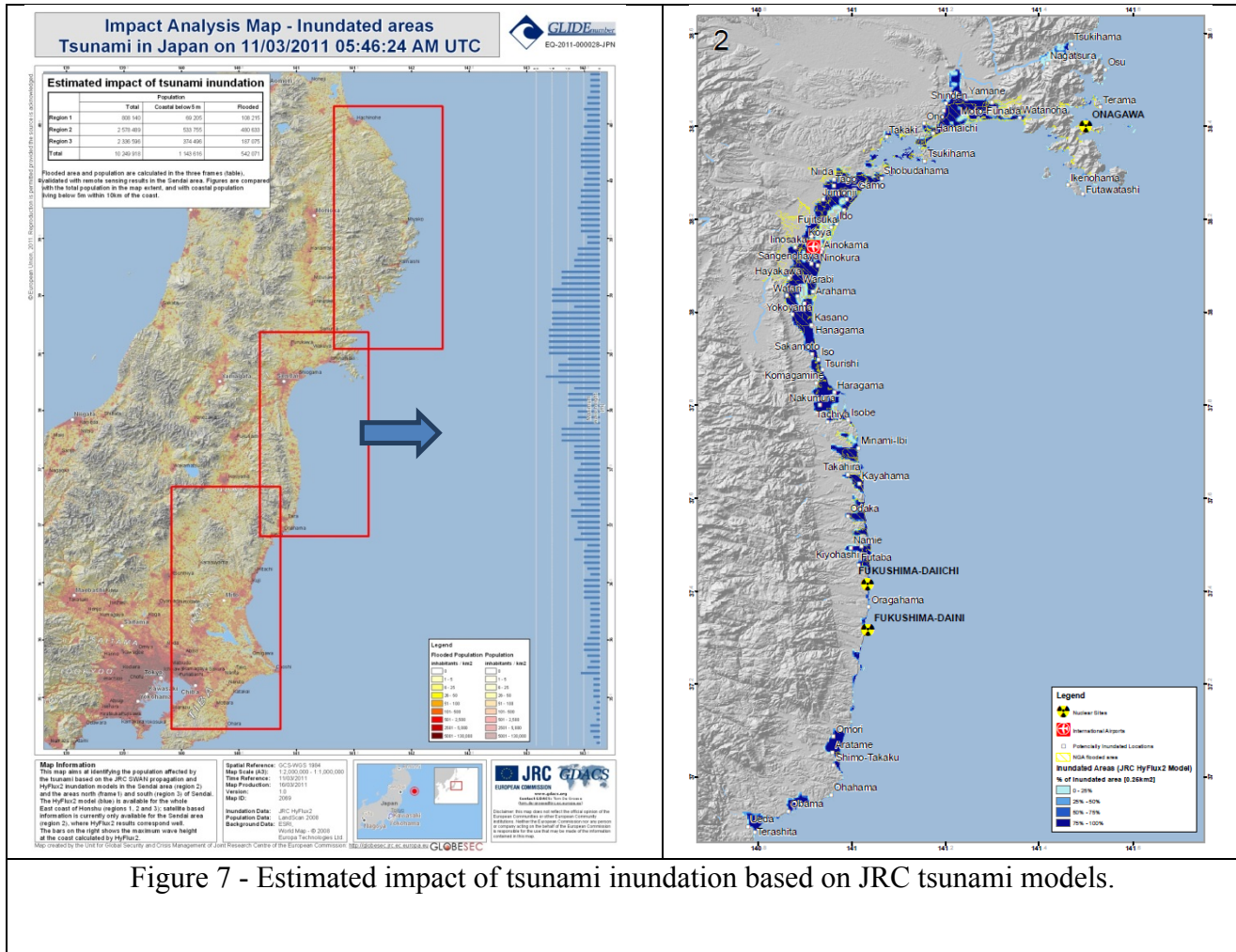


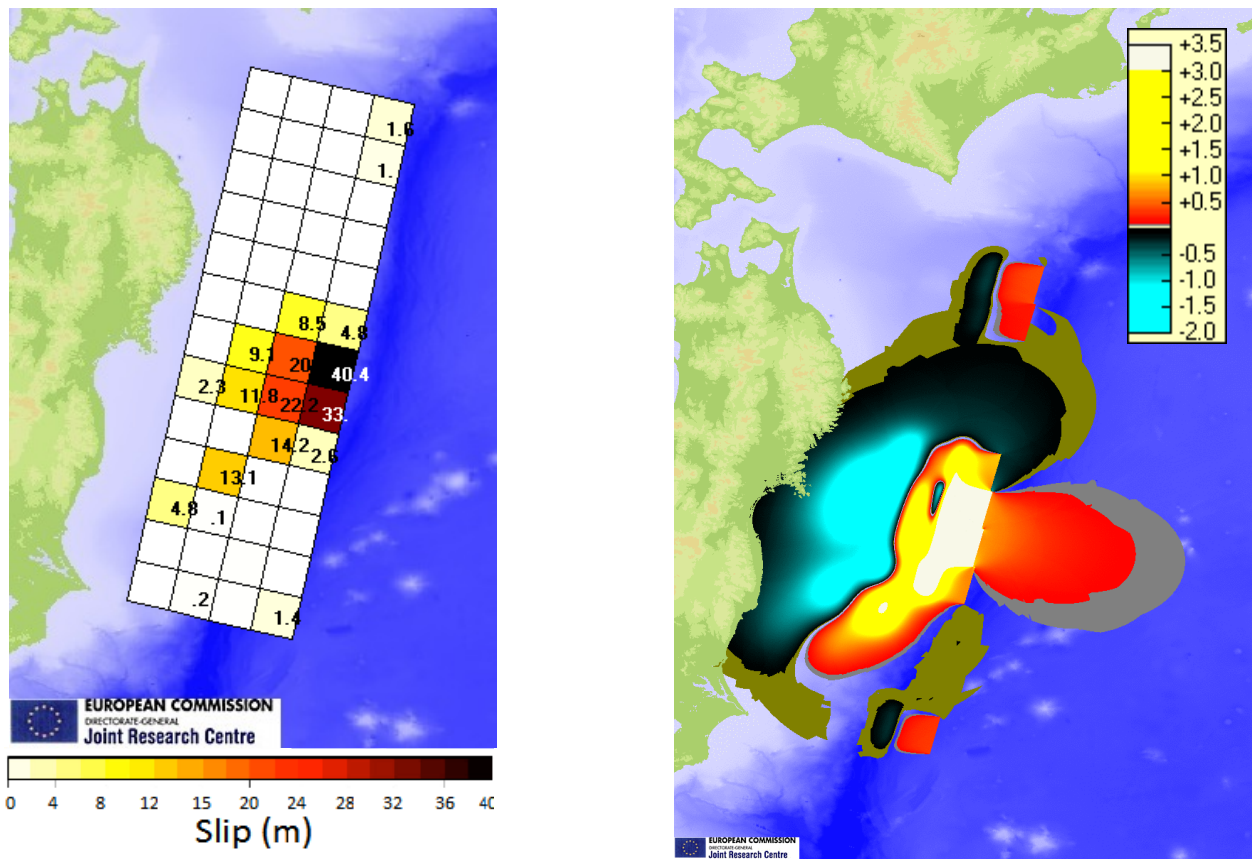
Figure 7 - Estimated impact of tsunami inundation based on JRC tsunami models.

### 4.3 Source estimation calculations

The large number of sea level measurements in Japan allows performing a very detailed estimation of the initial source (Figure 2); the ones used in this paper are 6 floating GPS, 10 tidal gauges, 2 cable pressure in addition to 3 DART stations provided by NOAA. The floating GPS are buoys equipped with GPS antennas whose signal is analyzed using reference GPS on land to perform a differential measurement; the cable pressure are submarine cables hosting at their end pressure sensor device.

The inversion was performed by creating a matrix of potential unit sources in the area in front of Japan and more specifically around the area that was subject to the aftershock events (Annunziato, 2012). In particular 52 potential faults with unitary slip (1 m) and width/length of 50x50 km have been considered; the additional parameters - strike  $193^\circ$ , dip  $14^\circ$ , slip angle  $81^\circ$  - are from the USGS's W-phase moment tensor solution.

The assumed depth of the faults are 0, 12, 25, 37 km going from the trench towards Honshu island in respect to the reported hypocentral depth. The initial deformation was calculated using the Okada model (1985) and the calculations have been performed using the SWAN-JRC code (Annunziato, 2007) with a grid cell matrix of 1080x1200, cell size of 30 arcsec (0.9 km), GEBCO bathymetry (IOC et al, 2003). In order to compare far distant measurements a coarser nodalization was also used: GEBCO re-sampled at 2 min (3.6 km) and 840x600 grid matrix. All the calculations have been carried out for a 2 hour simulation time.



Estimated slip with JRC Mod 1.0 (50x50 km)

Estimated initial sea level deformation

Fig. 8 – Slip obtained by inversion process and resulting sea level deformation

The form of the slip distribution shows that the fault extension is much smaller than the 500 km assumed for the simple single fault model (note that each square is 50 km and therefore the maximum length is in the order of 200-250 km). The smaller length means also a higher slip in order to respect the energy distribution. Also two sections are evident from the left part of Fig. 8 with a shallower and a much deeper section of the fault. This distinction is the one responsible of the double peaks shown in the data. The comparison of the result of the application of the source distribution obtained by the sea level measurements inversion is shown in the previous figures 4 and 5 and widely described in a paper under review (Annunziato, 2012).

## **5. DISCUSSION ON THE GDACS RESPONSE**

The analysis of the response of the GDACS system allowed drawing some conclusions, which then have led to changes in the automatic procedures.

The early values of the declared magnitudes, in particular for large events like this can be very much affected by the clipping of the instruments and therefore the estimation tend to increase over the time: this was true for Chilean event of 2010 and also for the 2011 event in Japan. This means that it is necessary to check as soon as possible the correspondence between the candidate scenarios with few measured sea levels to eventually correct the proposed magnitude. At this stage we do not find a reliable way to perform automatically this check and therefore we still leave this activity to the operators in charge of such analyses, if any. Nevertheless we are including procedures that allow the operator to react and report the feedback of his/her analysis on the estimates that are shown in the web site online (moderation activity).

The proposed fault mechanisms are very important in order to better describe an event and in some cases (Indonesia, April 2012) can show a completely different mechanism in respect to the one used for the calculations. This is why we are introducing in GDACS an automatic fault mechanism scraping that is able to detect the publication of a fault mechanism online and launch a new calculation that becomes part of the moderation process in the GDACS system.

The inundation calculations should be done automatically following an event and therefore we have now implemented a new calculation strategy so that for each online calculation a series of more and more refined calculations is launched in sequence in order to estimate, within 2 hours from the start of the calculation the inundation extent.

## **6. CONCLUSIONS**

The analysis of the response of the GDACS system to the Tohoku Earthquake has shown that the scenario matrix, which is the base for the alerting system of GDACS, is suitable to identify correctly the sea level impact of tsunamis if correctly initialized with the earthquake parameters. The early comparison with sea level measurements is also able to give indications on the quality of the

candidate scenario automatically selected based on the parameters, which are provided. Much better results can be obtained by the use of the true fault mechanism solutions, which are published a few hours after the event. The use of such data allowed to correctly estimate the sea level inundation in the case of the Tohoku event.

Finally the use of sea level inversion techniques allow to depict much better the real fault extent and its slip distribution, but at the moment it does not seem possible to apply such methods in real time for very detailed source distributions - but is useful to understand the deformation extent.

A number of improvements to the GDACS system are being implemented as a result of the analysis of the Japan event and of other important events that should make the system more reliable and useful for the users community.

## REFERENCES

Annunziato, A. (2005). Development and Implementation of a Tsunami Wave Propagation Model at JRC. Proceedings of the International Symposium on Ocean Wave Measurement and Analysis. Fifth International Symposium on Ocean Wave Measurement and Analysis.

Annunziato, A. (2007). The Tsunami Assessment Modelling System by the Joint Research Centre. Science of Tsunami Hazards 26:2, 70-92.

Annunziato, A. (2012). Estimation of the Tsunami Source for the 2011 Tohoku Tsunami – paper under review process.

De Groeve, T.: Global Disaster Alert and Coordination System: More Effective and Efficient Humanitarian Response, Proceedings of the 14th TIEMS Annual Conference, 324-334, Trogir, Croatia, 2007.

De Groeve, T., Peter, T., Annunziato, A. and Vernaccini, L.: Global Disaster Alert and Coordination System, [http://www.gdacs.org/documents/2009\\_GDACS\\_overview.pdf](http://www.gdacs.org/documents/2009_GDACS_overview.pdf), 2009.

De Groeve, T., Vernaccini, L. and Annunziato, A.: Modelling Disaster Impact for the Global Disaster Alert and Coordination System, Proceedings of the 3rd International ISCRAM Conference, May 2006, Newark, NJ (USA), 409-417, 2006.

Franchello, G. (2008). Modelling shallow water flows by a High Resolution Riemann Solver. JRC Scientific and Technical Reports. EUR 23307 EN 34p.

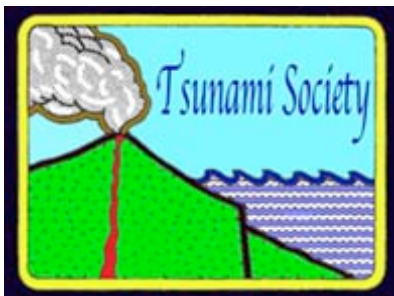
Franchello, G. (2010). Shoreline tracking and implicit source terms for a well balanced inundation model. International Journal for Numerical Methods in Fluids 63:10, 1123-1146.

Franchello, G. and Annunziato, A. (2012). The Samoa tsunami of 29 September 2009- Early Warning System and Inundation Assessment. *Science of Tsunami Hazards* 31:1, 19-612.

Y. Fujii, K. Satake, S. Sakai<sup>2</sup>, M. Shinohara, T. Kanazawa – ‘Tsunami source of the 2011 off the Pacific coast of Tohoku Earthquake’ – *Letter to Earth Planets Space*, 63, 815–820, 2011

Mader, C. (2004). *Numerical Modeling of Water Waves*. 2nd ed., CRC Press, Boca Raton, Fl. 274p.

ISSN 8755-6839



**SCIENCE OF TSUNAMI HAZARDS**

---

Journal of Tsunami Society International

**Volume 31**

**Number 4**

**2012**

---

*Copyright © 2012 - TSUNAMI SOCIETY INTERNATIONAL*

*TSUNAMI SOCIETY INTERNATIONAL, 1741 Ala Moana Blvd. #70, Honolulu, HI 96815, USA.*

[WWW.TSUNAMISOCIETY.ORG](http://WWW.TSUNAMISOCIETY.ORG)